

The Troodos ophiolite, Cyprus

A field trip guide

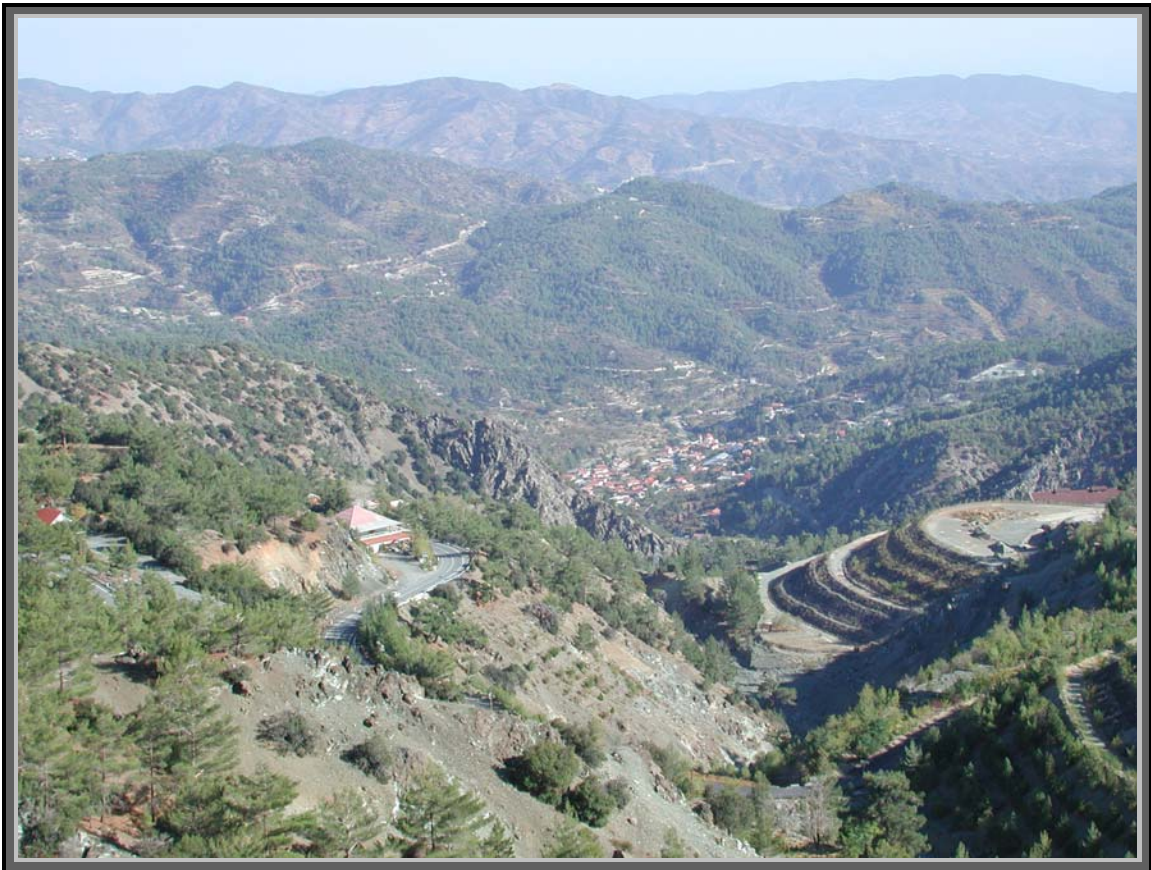
The *Geological Society of Israel*

May 2011

Tour leaders: Amotz Agnon (Hebrew University)

Yaron Katzir (Ben-Gurion University)

Meir Abelson (*Geological Survey*)

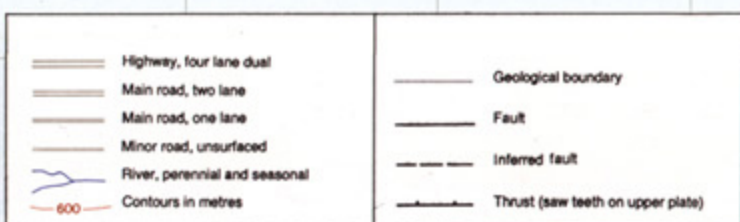
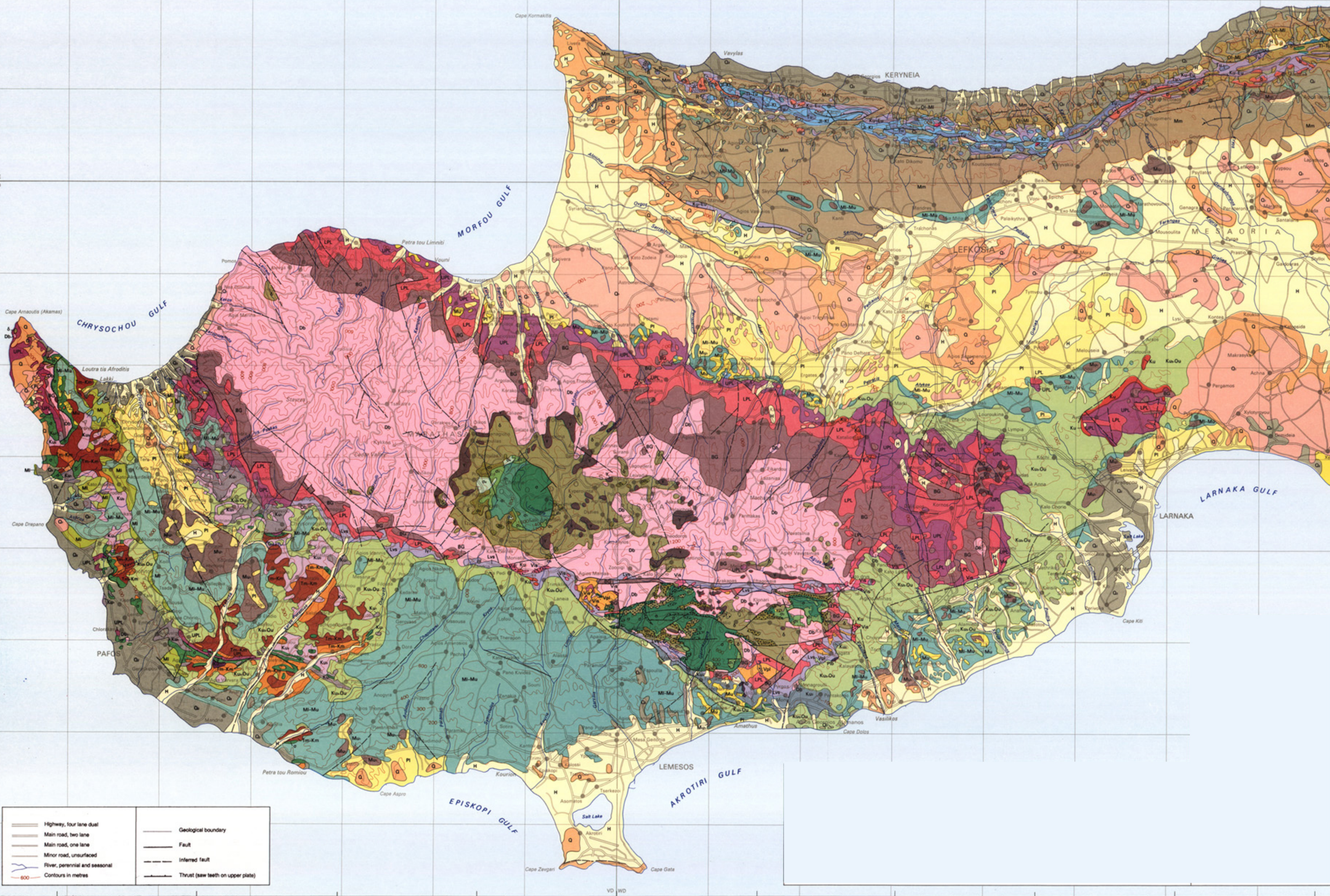
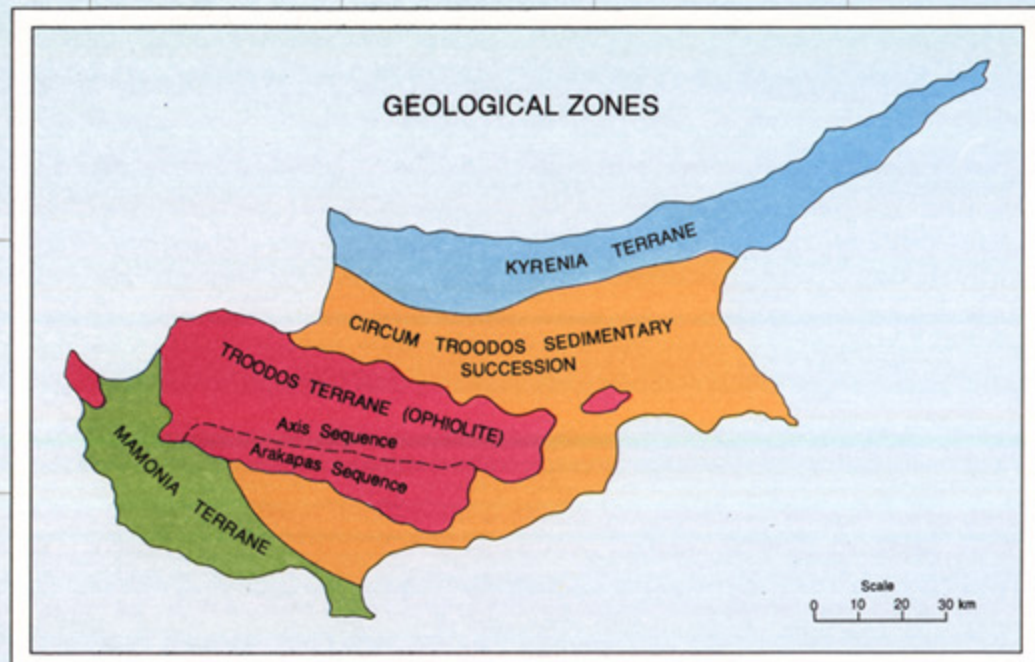


Edited by Meir Abelson, Yaron Katzir & Amotz Agnon

GEOLOGICAL MAP OF CYPRUS

SCALE 1 : 250 000
 km 5 4 3 2 1 0 5 10 15 20 km

Compiled, designed and drawn by the Geological Survey Department, Cyprus
 Director G. Constantinou, Ph. D. (London), D.I.C., M.I.M.M.
 Revised 1995



CIRCUM TROODOS SEDIMENTARY SUCCESSION

LITHOLOGY	FORMATION	EPOCH	PERIOD
H: Sands, silts, clays and gravels	Alluvium-Colluvium	HOLOCENE	QUATERNARY
Q ₁ : Calcarenes, sands and gravels	Terrace deposits	PLEISTOCENE	
Q ₂ : Gravels, sands and silts	Fanglomerate		
Q: Biocalcarenes, sandstones, sandy marls and conglomerates	Apalos-Athalassa Kakkaristra	PLIOCENE	NEOGENE
PI: Biocalcarenes, sandstones, silts, gravels, sandy marls, marls, limestones and conglomerates	Nicosia		
Mu: Gypsum alternating with chalky marls and marly chinks	Kalavasos	UPPER	
Mu: Biostrome and bioherm reef limestones (Koronia Member)	Pakhna	MIDDLE	
MI-Mu: Chalks, marls, marly chinks, chalky marls and calcarenites		LOWER	
MI: Biostrome and bioherm reef limestones (Terra Member)			
Ku ₁ -Ou: Chalks, marls, marly chinks, chalky marls with cherts in places as bands or nodules	Lefkara	OLIGOCENE EOCENE PALAEOGENE	PALAEOGENE
Ku ₂ : Variably coloured, poorly sorted debris with angular clasts upto boulder size in a sand and clay matrix. Most clasts are derived from the Mamonia Complex but some are of Troodos ophiolite lithologies	Kathikas	(Maastrichtian)	UPPER CRETACEOUS
Ku ₃ : Melange of older (Triassic-Cretaceous) blocks of yellow quartz sandstone, grey siltstone, serpentinite and other lithologies, entrained in a matrix of silt and bentonitic clay	Moni		
Ku ₄ : Bentonitic clays interbedded with off-white volcanoclastic sandstones	Kannaviou	(Campanian)	

TROODOS TERRANE (TROODOS OPHIOLITE)

OLYMPUS (AXIS) SEQUENCE	UPPER CRETACEOUS (Campanian)	UPPER CRETACEOUS (Upper Cenomanian - Lower Campanian)	
Ku: Hydrothermal and deep-water sediments; umbers, manganoan shales, pink radiolarian shales and mudstones	Perapedhi		
UPL: Olivine- and pyroxene-phyric, pillow lavas with occasional sheet flows, dykes, and hyaloclastites, commonly altered to zeolite facies	Upper Pillow Lavas		
LPL: Pillowed and sheet lava flows with abundant dykes and sills, altered to zeolite facies and in places stained with green caladonite	Lower Pillow Lavas		VOLCANIC SEQUENCE
BG: Diabase dykes (>50% with pillow lava screens, altered to greenschist facies)	Basal Group		
Db: Diabase dykes upto 3m wide, aphyric and clinopyroxene- and plagioclase-phyric altered to greenschist facies	Sheeted Dykes (Diabase)		INTRUSIVE SEQUENCE
Y: Trondhjemites, granophyres, diorites, quartz-diorites and micro-granodiorites	Plagiogranite		
δ: Isotropic gabbros, uraltite gabbros, olivine gabbros and layered melagabbros	Gabbro		PLUTONIC SEQUENCE
σ: Websterites, clinopyroxenites, orthopyroxenites, and plagioclase-bearing pyroxenites	Pyroxenite		
ω: Wehrlites and plagioclase-bearing wehrlites, massive or layered	Wehrlite		
ο: Dunites with subordinate clinopyroxene-dunites	Dunite	MANTLE SEQUENCE	
ο: Tectonized harzburgites with minor dunites and lherzolites	Harzburgite		
ο: Pervasively serpentinitized, tectonized harzburgites with minor dunites and lherzolites	Serpentinite		

ARAKAPAS (TRANSFORM) SEQUENCE

Pib: Angular pillow fragments supported by a matrix of brown-red iron rich mudstone	Pillow Breccia
Vis: Fine-grained interlava volcanogenic sediments: (a) sandstones, grits and silts interbedded with laminated iron and manganese-rich mudstones	Lavas and Volcanoclastic Sediments
Vps: (b) Coarse polymict breccias with lava, dyke and isotropic gabbro clasts	
Lvs: Olivine- and /or pyroxene-phyric, aphyric pillow lavas with some hyaloclastites, sheet lava flows and dykes, altered to zeolite facies	
Vpl: Vitrophyric pillow lavas, generally olivine-phyric and/or orthopyroxene-phyric	Intrusive Plutonic Rocks
Is: Isotropic gabbros, microgabbros and norites	
Wp: Poikilitic wehrlites and plagioclase-wehrlites	Sheared Serpentinite
Ss: Serpentinite in subvertical shear zones, 50-500m wide	

Introduction (taken from Cann et al., 2010)

The Troodos ophiolite

The Troodos ophiolite is a nearly intact mid-Cretaceous (91 Ma) slice of oceanic crust, exposed over an area of 40 by 100 km in the Troodos mountains of Cyprus and the foothills around them. Access by road to all parts of the ophiolite is straightforward. Troodos was one of the first ophiolites to be studied in detail and has had a profound influence on thinking about the ocean crust. For example, it was in Troodos that Ian Gass (Gass, 1968) first recognized that the sheeted dyke complex there was de facto evidence for seafloor spreading, and that ophiolites thus represent on-land fragments of oceanic lithosphere.

The Troodos ophiolite formed in a supra-subduction zone environment, as shown by lava geochemistry (Pearce, 2003), in a small ocean basin within the complex Tethyan ocean domain (Robertson et al., 1991). The spreading centre ran E-W at the time of crustal creation, but the ophiolite was rotated 90° anticlockwise soon afterwards, at the end of the Cretaceous. Now the general trend of the sheeted dykes runs N-S and the Arakapas Fault Belt, thought to be either a discrete transform fault or the northern edge of a broad transform-related domain, trends E-W. The low relief of the lava surface beneath the sedimentary cover (most of the fault scarps are less than 20 metres high) suggests that the spreading rate may have been greater than 60 mm/yr full rate, while the complexity of the gabbroic units suggests that the spreading rate was slow; an intermediate spreading rate seems a good estimate.

The ophiolite can be divided into three regions:

- 1) The main Troodos Massif north of the Arakapas Fault Belt, which preserves a Penrose-type ophiolitic stratigraphy, but with some complications,
- 2) The east-west Arakapas Fault Belt, interpreted as the northern margin of a fossil transform fault or as a discrete transform fault,
- 3) The Limassol Forest Complex, south of the Arakapas Fault Belt, in which similar lithologies to those of the main Troodos Massif occur, but in complex structural relationships with one another, including low-angle extensional faults. The interpretation of this area is subject to intense controversy.

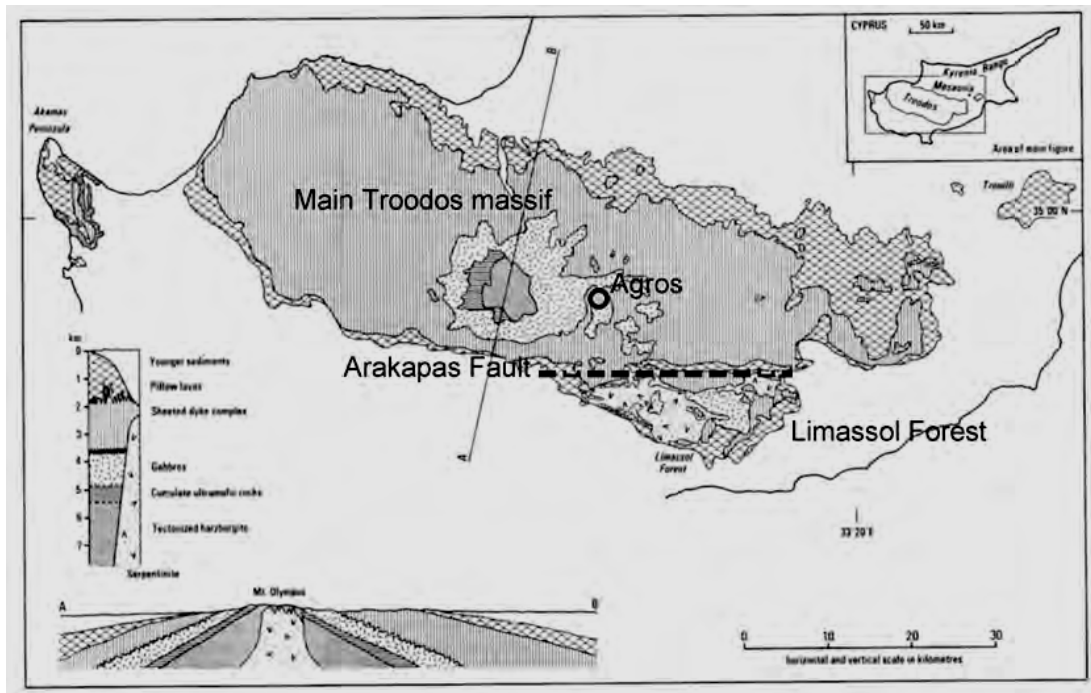


Figure 1: Outline geological map of Cyprus showing the three areas to be visited (adapted from Gass, 1980).

Troodos Massif

The overall lithostratigraphy of the main Troodos massif is relatively simple. Submarine volcanics overlie sheeted dykes that in turn overlie an upper plutonic unit composed principally of gabbros. This in turn overlies a unit of mantle peridotite. Sulphide deposits occur within the lava section and related deposits of unburnt overlie the lavas. The structure is dome-like so that the deepest parts of the stratigraphy occupy the central, topographically highest area (Fig. 1).

The **submarine volcanics** show a wide range of volcanic products (Schmincke and Bednarz, 1990). These include pillow flows, sheet flows, breccias and hyaloclastites. Compositions range from basalts through to andesites, dacites and rhyolites, and include lavas allied to boninites (distinctive high-magnesium andesites otherwise found in intraoceanic forearcs). Individual lava flows can be identified and traced for several kilometres along strike. The lavas are cut by faults that displace the ocean floor only by tens of metres, but are associated in places with rotation of the dip of the lavas, which can be shown to have happened at the spreading axis. The thickness of the lavas is variable, but is typically about 1000 m.

Over much of its thickness, the **sheeted dyke** unit can be shown to be made up entirely of dykes intruding one another, a graphic demonstration of ocean floor spreading. The dykes range in width from narrow veins up to over ten metres, but the typical range of widths is from one to about five metres. Though some dykes intrude high into the lavas, the main transition from lavas to sheeted dykes happens over a vertical distance of only 100–200 m, as has been observed in oceanic drill holes, indicating crustal construction from a narrow zone of dyke injection (Kidd and Cann, 1974). Over much of the Troodos massif the dykes trend approximately north-south, indicating the orientation of the spreading axis during crustal construction. The direction of magma intrusion in the dykes varies from vertically upwards to horizontal, or sometimes even downwards (Staudigel et al., 1999). The dyke trend swings round to NE-SW and locally E-W towards the Arakapas Fault Belt. Palaeomagnetic data and cross-cutting dykes suggest that this is the result of clockwise rotation, soon after the dykes were formed, induced by dextral shear along the transform. The sheeted dyke complex is extensively deformed by brittle fracturing and generally metamorphosed in the greenschist facies.

Below the sheeted dykes, the **upper plutonics** are composed principally of layered and unlayered gabbro, with some ultramafic layers and veins and pods of plagiogranite, apparently the result of extreme fractionation of basaltic magma. The plagiogranites are in places highly altered to epidote-quartz assemblages, apparently generated by magmatic fluids (Kelley and Malpas, 1992). The unit has a complex structure, with multiple intrusive relationships that can well be seen in the field (Malpas 1990). At least three distinct relationships between dykes and gabbros have been described in the Troodos Massif. At some localities the transition is gradual over a few hundred metres, with vertical dykes separated by gabbro screens becoming thicker and coarser grained downwards, while still showing chilled margins. Elsewhere there is a sharp boundary, with the gabbros intruding and metamorphosing the dykes (Gillis and Coogan, 2002) (as described from ODP Hole 1256D). Finally there is an extensive area in the NW where dykes rotated to low angles are separated from gabbros by a low-angle brittle fault, the Kakopetria detachment.

The hotel in Agros lies within the upper plutonics. Gabbros outcrop just beyond the hotel grounds. North of the hotel there is an excellent view of a gabbroic ridge capped by sheeted dykes (Fig. 2).

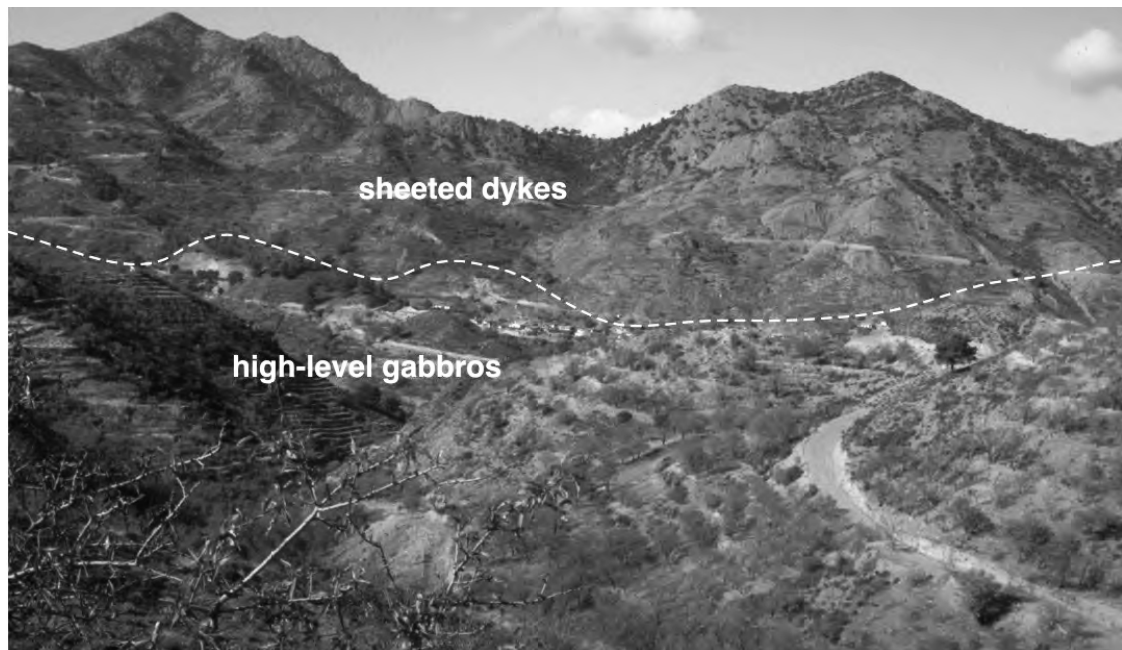


Fig. 2 Gabbro-dyke boundary above Agros

The **lower plutonics** are dominated by ultramafic and, to a lesser extent, gabbroic rocks, often layered. They grade downward into pyroxenites and massive dunites that form a thick crust-mantle transition zone.

The **upper mantle**, composed of partially serpentinized harzburgite, dunite and pyroxenite, is exposed around the peak of Mount Olympus, and there are excellent localities showing evidence of percolation of magma through mantle harzburgites. Chromite was mined from the mantle section, and the relationships can be seen between chromite ore and host mantle. Peridotite pervasively altered to serpentine forms a 'bull's eye'-shaped unit at the east side of the mantle exposure. The formation of this unit is controversial. Its chromites have distinctly different compositions to all other Troodos peridotites. The circular outcrop is underlain by a large negative gravity anomaly, constraining the body to have a pipe-like form. It is conventionally regarded as being the result of doming during uplift of the ophiolite during the Neogene, probably linked to diapiric intrusion related to volume increase during hydration. However, it has recently been suggested that the steep reverse fault that bounds the east side of the serpentinite (the Amiandos Fault) was the steep part of an oceanic detachment fault formed during crustal construction, possibly connecting with the shallow Kakopetria Detachment (see below) between the dykes and the gabbros. We will visit exposures of the Amiandos Fault on the second day of the excursion. In places within massifs of serpentinite both in the main Troodos area and in the Limassol Forest, there are springs of cool calcium-rich, alkaline fluids produced during continuing serpentinization of the peridotite. These springs are analogous to the Blue Pool springs of Oman and the Lost City vents at 30°N on the Mid-Atlantic Ridge.

During crustal construction, **black smoker circulation** was common. Pyrite-rich exhalative sulphide deposits occur within the lavas at different levels, and were mined for copper and/or sulphur. Their exhalative nature can be demonstrated by associated sediments formed by seafloor weathering of the sulphides, and by the presence of fossil worm tubes and gastropods within the sulphides. Beneath the sulphide deposits are alteration pipes that reach down to the top of the sheeted dyke unit through which hydrothermal solutions rose to the seafloor. Near the base of the sheeted dykes are extensive high-temperature hydrothermal reaction zones marked by development of epidiosites (epidote-quartz rocks) within the dykes, and by depletion in Cu, Zn, and Mn (Richardson et al., 1987; Varga et al., 1999). The black smoker circulation took place very close to the ancient spreading axis, as can be shown by the burial of almost all of the sulphide deposits within the lava pile, by the close association of the hydrothermal reaction zones with the dyke-gabbro boundary, and by field evidence that dykes were being intruded while hydrothermal circulation was proceeding.

Iron and manganese-rich **hydrothermal sediments (umbers)** occur in many places on top of the lava sequence, and occasionally within it. Within hollows or in half-grabens their thickness may reach 35 metres, but most deposits are less than 10 metres thick. These sediments are interpreted as fallout from black smoker plumes, formed by oxidation of the iron sulphide black smoke particles in the water column and by adsorption of hydrothermal manganese from the diluted hydrothermal solutions onto the newly formed iron oxides. They subsequently accumulated on the seafloor and were preserved in hollows in the seabed. By analogy with modern systems, accumulation rates of the umbers were probably fastest close to the vents, and just beyond the limit reached by lava flows, though accumulation may have continued for several million years at ever-decreasing rates as the crust spread away from the spreading centre.

Low-temperature circulation continued for several tens of millions of years after crustal construction. This has been documented by K/Ar dating of low-temperature alteration minerals such as celadonite (Staudigel et al., 1986). In areas where the seafloor was not covered by sediment for a long time, low-temperature circulation produced oxidative alteration of the basalts with the development of orange palagonite and carbonates (Gillis and Robinson, 1990). Deeper in the section in these same areas, alteration becomes more reducing and less pervasive, so that fresh basaltic glass remains in pillow margins. As temperature of alteration increases with depth, it can be difficult to distinguish later alteration from early black smoker alteration once the sheeted dyke complex is reached.

Several **structural grabens** have been identified in the main Troodos massif, mainly by the rotation of dykes in the sheeted dyke complex. The most marked one of these is the Solea Graben that we will be visiting on the first and second day trips. On either side of this the dykes dip towards the graben axis, implying rotation in the hangingwall caused by ‘bookshelf’, probably listric, faulting above a low-angle fault located at the gabbro-dyke boundary (Varga 1991, Hurst et al., 1994). This low-angle structure has been termed the ‘**Kakopetria Detachment**’. The rotation is especially large on the west side of the graben axis, where the dykes may dip at less than 30° towards the east. This rotation can be shown to have happened very early in the history of the ophiolite, during the construction of the oceanic crust, but after the epidotisation that happened very soon after dykes were intruded. These and other structural observations have led the Solea graben to be interpreted as an extinct spreading axis within the ophiolite, though its overall morphology is rather different from extinct spreading axes in the oceans. It is clear that this region has seen major extension, and an important question is whether this extension is or is not related to detachment faulting of the type seen in the oceans. The lack of displacement of the uppermost lavas by the faults within the grabens, and the lack of significant mass wasting deposits in the lava sections, is hard to reconcile with the large rotations of the dykes. These relationships are apparently at odds with observations from slow spreading ridges, such as the Atlantic, where large fault-related rotations have been observed.

Arakapas Fault Belt

The Arakapas Fault Belt runs east-west along the southern edge of the Troodos massif. It forms a prominent linear valley that is clearly visible today, on the ground or from space. The fault belt is about 1 kilometre wide and was identified as a **transform fault** by Moores and Vine (1971). It runs at right angles to the dyke trend and is blanketed by overlying pelagic sediments, so was clearly an ocean-floor structure. Soon after, Simonian and Gass (1978), showed that the fault belt formed a topographic trough at the time the ophiolite was forming. The basement of the fault zone is made of highly deformed and metamorphosed sheeted dykes. Part of the fill is of lavas, most of which belong to a geochemically distinctive boninitic lava series with highly depleted compositions and U-shaped rare-earth element profiles. These lavas are generally unaltered, with abundant fresh glass. The other component of the fill is sedimentary. The sediments are interbedded with the lavas and range from proximal coarse polymictic breccias to turbiditic sandstones and fine-grained sediment dominated by reworked umber. The breccias contain clasts of lava, diabase from the sheeted dykes and very rare fragments of microgabbro. These indicate considerable relief on the walls of the transform valley but not enough to expose mantle rocks or the main plutonic sequence. The fill of the trough is locally cut by fault strands, but is otherwise significantly less deformed than the basement.

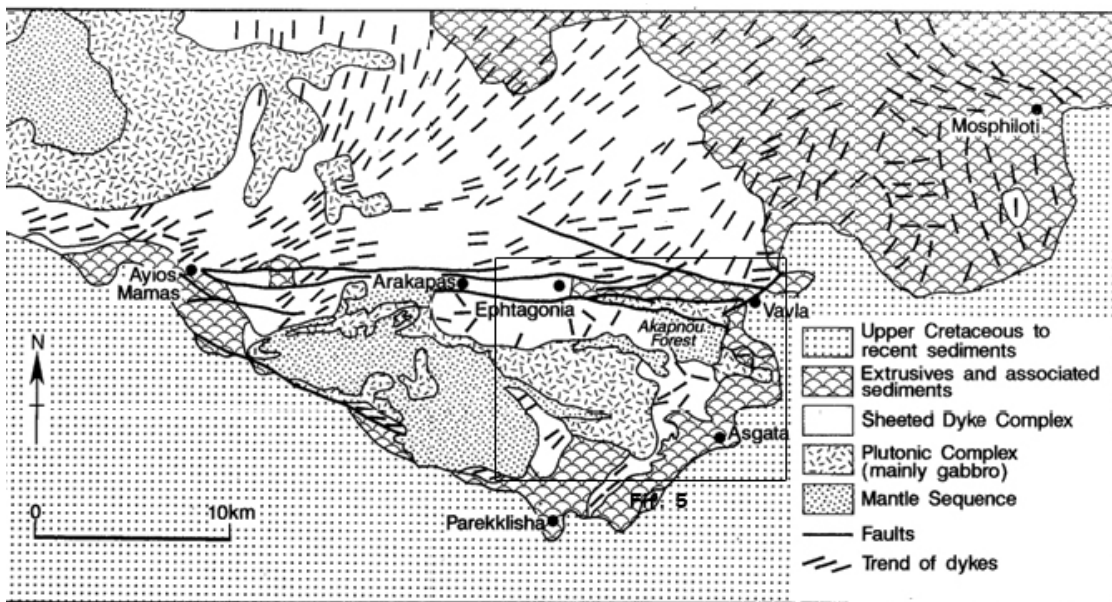
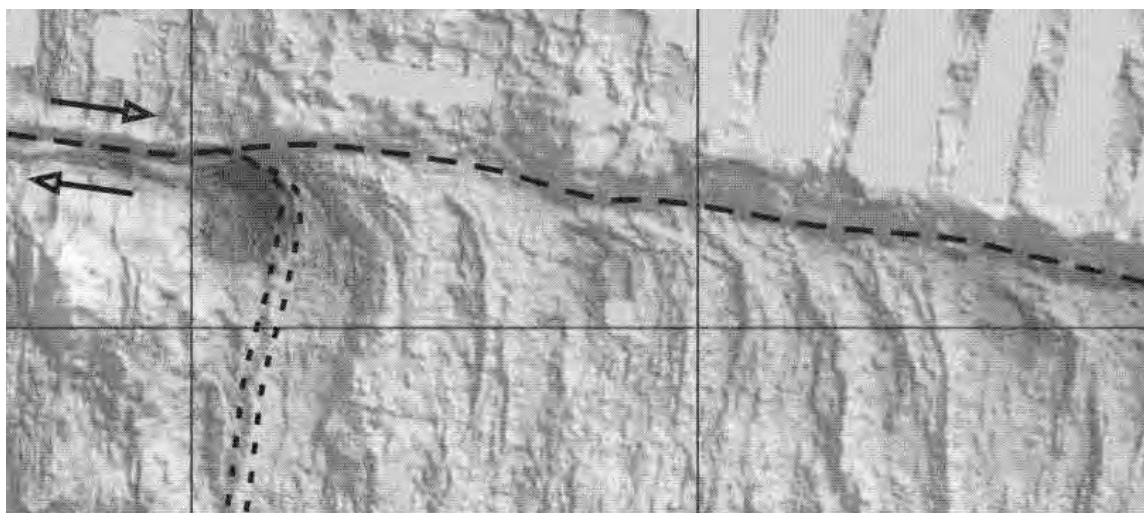


Fig. 3. Geological map of the Arakapas transform fault and the Limasol Forest Complex



Volcanic ridges near the Kane Fracture Zone 0 — 10 km
 Fig. 4. Side scan image of an active ridge-transform intersection near the Kane FZ in the Mid-Atlantic Ridge.

At many modern transforms the trends of the volcanic ridges and faults created at the spreading axis curve progressively towards the opposite ridge crest as the fault is approached (the ridge offset being in the opposite sense to the slip direction on the transform fault). This swing in direction is usually taken to be caused by rotation of the stress field from extensional to strike slip as the fault is approached, and the formation of extensional faults and dykes in this rotated stress field. In the Troodos Massif, the strikes of the dykes and faults swing progressively from north-south to NE-SW as the Arakapas Fault Belt is approached, on much the same scale as the deviation of abyssal hill trends in the oceans. By simple analogy with modern transform systems this dyke swing should therefore imply dextral offset of the ridges and sinistral slip along the Southern Troodos Transform Fault Zone. However, this analogy raises a conundrum, as steep serpentinite shear zones within the Limassol Forest Complex show kinematic indicators of dextral strike-slip movement. Palaeomagnetic measurements from NNE- to NE- to ENE-trending dykes in the area of dyke swing in Troodos demonstrate clockwise rotations about vertical axes, clearly showing that the deviation of dyke trend was caused by the bodily rotation of dykes subsequent to their intrusion, rather than by intrusion of dykes into a rotated stress field (Bonhommet et al., 1988; Allerton and Vine, 1990; Morris et al., 1990). This, however, raises an interesting question: why should the swing of dyke trends in Cyprus be opposite to the sense normally seen in the oceans? Does this imply greater coupling across the Southern Troodos Transform Fault than at modern oceanic transforms? We cannot answer these questions definitively, but do note that in very rare cases at modern transform faults (e.g. Clipperton, Bullard) the block rotation sense of curvature is observed, i.e. abyssal hill fabrics swing inwards towards the (orthogonal) ridge-transform intersection.

Limassol Forest Complex

The Limassol Forest Complex lies south of the Arakapas Fault Belt. It contains the same lithological units as the Troodos Massif, but without the simple layered stratigraphy seen there; instead, the units are juxtaposed in a complex way, with very significant levels of brittle faulting. The area was first mapped (at 1: 5000 scale) and investigated in detail in the mid-1980s by Bramley Murton and Chris MacLeod (both PhD students of Ian Gass), in the western and eastern halves of the region, respectively. This work formed the basis of the Cyprus Geological Survey Department Memoir No. 9 (Gass et al., 1994) and accompanying 1: 25,000 scale geological maps. In the eastern Limassol Forest a wide range of crustal units, ranging from lower crustal plutonics up to sheeted dykes and lavas, is in direct contact with serpentinite with large parts of the crustal section missing over much of the area. These gaps in the stratigraphy suggest the presence of large-scale extensional faulting. The northeastern Limassol Forest, centred on the Akapnou Forest region, shows a basement unit of serpentinitized harzburgites and dunites overlain tectonically by overlapping, crustal blocks bounded by gently SW dipping normal faults. The boundary between the serpentinites and the tilted crustal blocks is a low-angle extensional detachment fault, termed the **Akapnou Forest Décollement** by MacLeod

In the western Limassol Forest (Excursion day 4) significant areas of serpentinitized mantle rocks are exposed as a number of domes, elongated east-west, juxtaposed by extensional faults against disrupted remnants of a layered crustal sequence, including gabbros, sheeted dykes and in places lavas. Large parts of the crustal section are missing. Major vertical serpentinite shear zones trending predominantly east-west with dextral strikeslip shear indicators cut the serpentinite. Some of these are up to 500 m in width and may be traced along strike for more than 5 km. Ultramafic and mafic plutons,

together with associated (usually NE-trending) dykes, cut the serpentinised mantle sequence and disrupted crustal blocks. Most of the dykes have been partly replaced by greenschist facies minerals and/or rodingitised. The plutons are composed of gabbro and wehrlite and have been much less serpentinised than the mantle harzburgite and dunite that form the basement. The dykes share the distinctive boninitic compositions with U-shaped rare-earth element patterns of the lavas erupted within the Arakapas Fault Belt. Because of their geochemical similarities with the lavas of the Arakapas Fault Belt, these were termed 'Transform Sequence' magmas by Murton, and interpreted by him as have been intruded syn-tectonically into the active domain of a broad **Southern Troodos Transform Fault Zone** that would stretch south from the Arakapas Fault Belt. The sequence and style of intrusion, and of alteration grade, is consistent with progressive cooling and uplift during the syn-tectonic magmatism in the western Limassol Forest. At the southern edge of the western Limassol Forest, clasts of serpentinite are found in sediments interbedded with lavas faulted against serpentinite. This indicates that serpentinite was already exposed at the sea floor at the time of the eruption of the lavas. The western part of the Limassol Forest has mostly been eroded to deeper levels than in the east following Miocene uplift (see below), but there are places where a similar low-angle fault that separates serpentinite beneath from sheeted dykes above have recently been identified. The low-angle faults demonstrably postdate and truncate the steep serpentinite shear zones. The low-angle faulting in the western Limassol Forest has not yet been investigated in any detail, but it may well represent a previously unrecognised continuation of the Akapnou Forest Décollement.

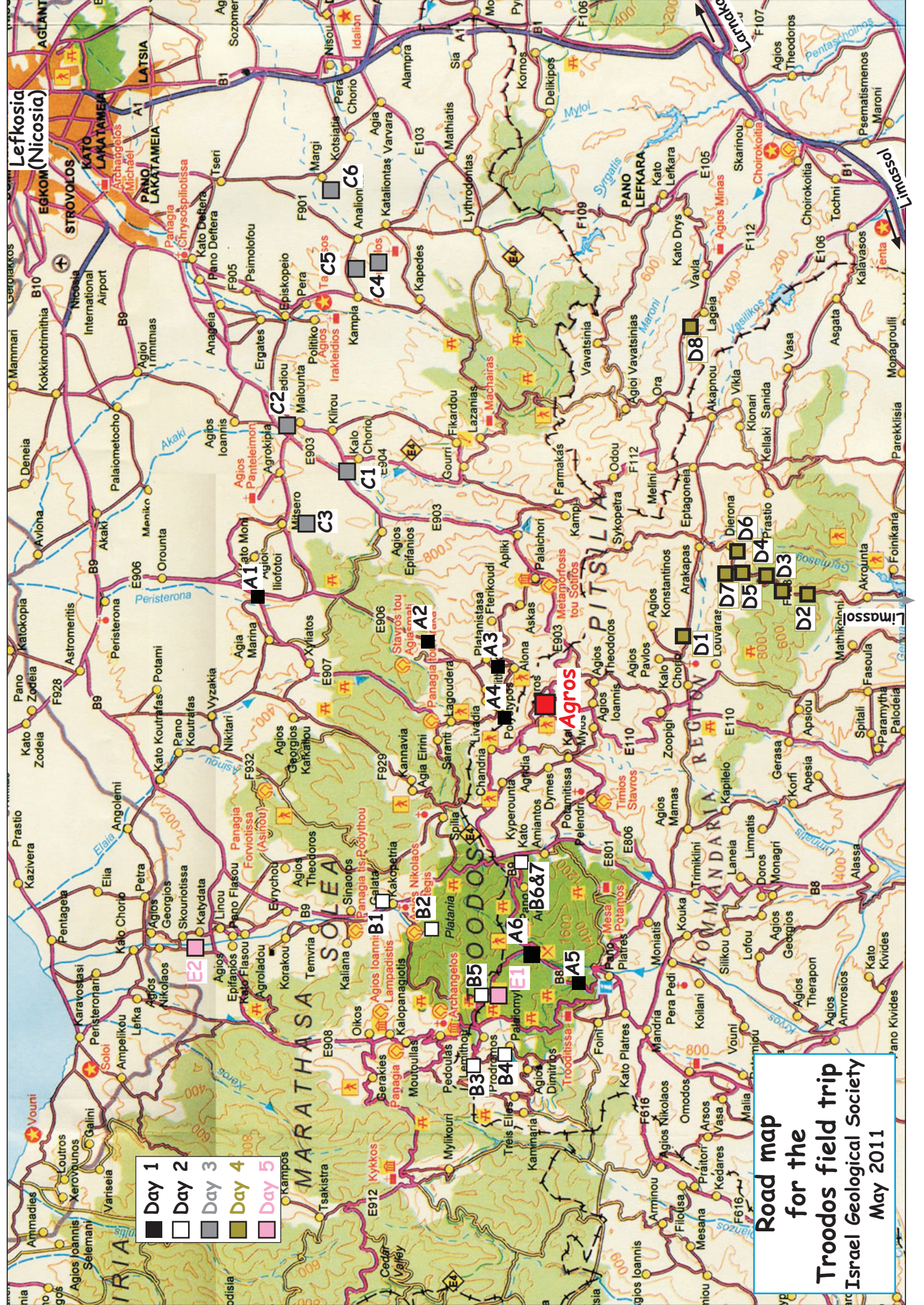
In the eastern Limassol Forest, north of the Kalavassos Mines region, clastic sediments are interbedded with volcanics, though south of the Kalavassos Mines such interlava sediments disappear. Deformation of this southern area is also significantly less than anywhere else in the Limassol Forest Complex, such that the ~45km² area of volcanics and (NE-trending) sheeted dykes exposed in the southeastern corner of the Limassol Forest massif is similar in overall appearance to upper crustal sequences of the main Troodos Massif. These observations together led MacLeod to conclude that the volcanics and (NE-trending) sheeted dykes exposed in the southeastern Limassol Forest (and probably also those disrupted crustal blocks in the remainder of the Limassol Forest) were generated at an '**Anti-Troodos**' ridge axis, on the opposite side of the transform zone from the main Troodos Massif. Palaeomagnetic studies of the NE-trending dykes in this Anti-Troodos region are consistent with early clockwise rotations about steeply-plunging axes. These rotations may have been induced by drag adjacent to a dextral transform and, as such, to be directly analogous to the dyke swing north of the Arakapas Fault Belt.

Tectonic interpretation of ocean-floor processes in the Limassol Forest area is made (even!) more difficult by several later deformation episodes. WNW-trending extensional structures cut the Akapnou Forest Décollement and rotated crustal blocks in the eastern Limassol Forest, and were reactivated as dextral strike-slip faults in the south at the same time as the Troodos microplate was rotated anticlockwise in the Campanian-Maastrichtian. A WNW-trending Miocene fold and thrust belt – probably reactivating late Cretaceous lineaments – runs along the southwestern margin of the massif, and locally results in serpentinites being thrust over Palaeogene chinks. This deformation is associated with the first stages in the uplift of the ophiolite – which was initially centred on the Limassol Forest block – and post-dates crustal construction by over 60 million years. Though the effects of this Miocene deformation are most significant in the southwestern Limassol Forest, reverse faulting is also present around the periphery of the Akapnou Forest serpentinitised peridotite massif in the northeastern Limassol Forest. The latest identifiable generation of faults – north-south trending extensional structures, some associated with gypsum – cut the Akapnou Forest Décollement and further complicate the geology of the Limassol Forest. Such structures also cut recent river terraces nearby and are present elsewhere in Cyprus (e.g. the Polis graben at the western end of the island), attesting to a phase of deformation that probably continues to the present day. The effects of all these later deformation episodes need to be carefully assessed and accounted for when attempting to interpret the ocean-floor tectonic processes operating here.

Transtensional structure vs. oceanic core complex – A controversy on the tectonics of the Limassol Forest Complex

The interpretation of the tectonics in the Limassol Forest is controversial. The original mapping of the area was by Chris MacLeod and Bramley Murton. Their conclusions have evolved slightly since some of their earlier papers (e.g. Macleod and Murton, 1993). In essence Chris and Bram's current view (in brief) is that the Southern Troodos Transform Fault Zone became a transtensional structure, whilst in the active transform domain, thus focusing the boninitic magmatism there. This probably occurred in response to a change in regional spreading direction, as the latest sheeted dykes in the main Troodos Massif are NW-SE trending. They envisage the Akapnou Forest Décollement as forming very soon afterwards, immediately post-dating the (local) crustal construction of the ophiolite, in response to continued stretching that pulls the Troodos and Anti-Troodos domains apart. Critically, to them, the Akapnou Forest Décollement develops in response to NE-SW extension, and the rotated bookshelf faults that bound the klippe in the hanging wall are reactivated, originally *transform* parallel structures.

The alternative view is that of Joe Cann and his colleagues (Cann et al., 2001) which has also evolved since publication. Currently his view (also in brief) is that the detachment faulting is related to the generation of oceanic core complexes by spreading-direction parallel extension *during* crustal construction, though the detachment faults may have been reactivated at a later date. The spreading-parallel faults in the west Limassol Forest would then be related to exhumation of core complexes and not to transform tectonics. The presence of serpentinite clasts in interlava sediments is evidence for early exposure of serpentinite at the sea floor, and hence for an early start to the tectonics of the area. This conclusion is supported by the metamorphism of dykes intruded into the serpentinite, indicating a host rock still hot from the mantle. The detachment faults would then have capped core complexes, though not all would have been exposed at the sea floor, and would, as in modern core complexes, have rolled over to steep dips close to transform faults. Later reactivation would explain many of the other observations.



- Day 1
- Day 2
- Day 3
- Day 4
- Day 5

Road map
for the
Troodos field trip
Israel Geological Society
May 2011

The Troodos field trip itinerary

Day 1 - An introduction of an oceanic lithosphere exposed in the Troodos ophiolite

During this day trip we will visit some key sites representing the various layers of the oceanic crust and some ultramafic rocks from the mantle. We will start with the upper layer, the volcanic rocks, and will go deeper into the oceanic lithosphere, through the sheeted dikes, gabbro, and ultramafic rocks of the mantle.

Stop A1 (Cann et al., 2010) - This stop demonstrates the variety of volcanic products formed by submarine eruptions in the Troodos ophiolite. The volcanic products are columnar-jointed sheet flow, pillows and hyaloclastite, a sandy sediment composed of clasts of volcanic glass, perhaps formed by submarine fire-fountaining, perhaps by the successive fragmentation of a slowly flowing, highly viscous (probably siliceous) lava. Farther west the pillow unit contains a single columnar-jointed sheet flow over the tops of the pillows, showing that it is not a sill. Continuing west, the pillows become brecciated and oxidised in a wide damage zone in the hanging wall of a major E-dipping fault. The fault dips to the east and the fabric in the fault zone shows that it is a normal fault. The oxidation of its hanging wall shows that it has been a conduit for low-temperature fluid flow.

Stop A2 (Cann et al., 2010) - About 5 km beyond the road junction, stop at a tall east-west road cut deep in the sheeted dykes (0505822, 3871448 [*0505857, 3871621*]). Here the sheeted dykes are very well-developed and relatively undeformed. First, examine the rocks closely to recognize the chilled margins of the dykes (many of the vertical cracks in the outcrop are not chilled margins, but joints).

Stop A3 (Cann et al., 2010) - About 1 km beyond Platanistasa, stop at an outcrop of the gabbro-dyke contact in a new road cut (0503866, 3866245 WGS 84 [*0503901, 3866418 Euro 1950 – map*]). The contact here, as in many other places, is clearly intrusive, with the sheeted dykes metamorphosed by the gabbro and truncated by it. The field relations are not easy to see at a glance. The sheeted dykes here have been rotated to dip at a shallow angle (350°/55°E). They have a granular, hornfelsic texture and the chilled margins of the dykes are recrystallised. Farther down the road towards Platanistasa the dykes are more extensively recrystallised and cut by veins of plagiogranites that may be partial melts of the hydrous metabasalt. These contain angular fragments of the dykes. Nearby are outcrops of coarse-grained gabbro.

Stop A4 (Malpas et al., 1998; Abelson et al., 2002) – This outcrop displays layered, cumulate gabbros which vary from melanocratic, olivine bearing through mesocratic pyroxene gabbros, to leucocratic layers all of which vary from 10 cm to 2.5 m in width. The stratigraphic position of the layered gabbro is close to the sheeted dike complex, therefore we are looking at high-level layered gabbro. The whole sequence is intruded by a clinopyroxene-phyric diabase dike, 1 m in width, which dips 70°E. The dike appears to be chilled on both margins. Paleomagnetic measurements suggest that the tilt of the gabbro layers (45°/178°) are original, at least from the cooling stage crossing the blocking temperature (580°C) (Abelson et al., 2002). The Anisotropy of magnetic susceptibility (AMS) shows that the gabbro minerals are imbricated to the gabbro layering in a sense of indication melt flow southward, towards the Arakapas transform (Abelson et al., 2001).



High-level, cumulate layered gabbro intruded by a diabase dike near the village of Lagudhera

Stop A5 (Malpas, 1987; Cann et al., 2010) – Low level layered gabbro. This cumulate gabbro is deep in the crust, deeper than any gabbro seen elsewhere. The dark and light layering arises from alternations of cumulate wehrlite and gabbro. Though the outcrop appears undeformed at first sight, the layers contain a variety of deformation features including tight recumbent isoclinal folds. The preferred orientation of the pyroxene and plagioclase is sub-parallel to the layering as well as axial planes of isoclinal folds.

Stop A6 – We will walk from the junction of the Troodos tourist center to see harzburgites with tectonic layering intruded by pyroxenite dikes and cracked by serpentinized joints.

Day 2 - The Solea extinct spreading axis and asymmetric tectonic extension - Implications for a fossil ridge-transform intersection (RTI) & oceanic core complex

During this day we will tour around the Solea paleo-spreading axis and follow the signs of tectonic extension and detachment faulting. We will discuss the possibility for a fossil oceanic core complex, a mechanism that bring deep seated rocks from the mantle and the lower crust towards the seafloor. This mechanism has a central role in the construction of oceanic crust in active slow spreading centers.

Stop B1 – Highly rotated, flat lying dikes near the town of Kakopetria. The rotation of the dikes occurred during spreading with a major component of tectonic extension.



Flat lying dikes near Kakopetria

Stop B2 – A segment of the Amiantos fault juxtaposing ultramafic rocks (mantle) against gabbro (lower crust). This fault was active during seafloor spreading and was probably the steep segment of a detachment fault of an oceanic core complex (Nuriel et al., 2009).



A panoramic view across the Amiantos fault in Stop B2

Stop B3 – The Lemithu detachment. This stop demonstrates a low-angle fault beneath highly rotated sheeted dykes on the west flank of the Solea Graben.



Detachment faulting in the Solea graben: highly rotated dikes (rotation about horizontal axis) overlying a gabbro near the village of Lemithu

Stop B4 – An outcrop of a plagiogranite (trondhjemite, *see glossary*) near the village of Palemylos.

Stop B5 – Plastic flow textures within dunite and harzburgite cut by pyroxenite veins. In general, the relationships between these rock types arise from the complex processes that take place during mantle melting beneath the spreading axis. The mantle is sheared as it rises and melts. Magma is removed from the rock, and also rises through the rock from the mantle beneath that has already started to melt. Dunite is generated by reaction between melt and the wall rock, and from olivine precipitated from the rising magma. The pyroxenite veins are characteristically and straight-sided – they postdate the fabric in the harzburgite but are cut by dunite veins.

Stop B6 – On the road between Troodos and Kakopetria above the asbestos mine of Amiantos, a segment of the Amiantos Fault (see Stop B2) juxtaposing fully serpentinized peridotite against gabbro of the lower crust. The isotopic signature of the serpentinites in this segment indicate ophiolitic rather than a spreading environment, i.e., a 2nd phase of serpentinization.

Stop B7 – Near stop B6 on a ridgeline observing the Amiantos mine, folded and banded wehrlites and pyroxenites are cut by pegmatitic gabbro, indicating a deformation of spreading environment of the ultramafic near the Amiantos fault.

Day 3 - The upper crust: lavas and hydrothermal deposits

The Akaki river canyon offers one of the best-exposed cross-sections through the extrusive series (1.7 km thick) of the Troodos ophiolite. Pillows are the dominant extrusive form in the upper part, sheet flows and pillows in the middle and sheet flows, pillows and extrusive breccias in the lower part of the section. Dyke density decreases abruptly above the lower part.

Stop C1a - Overview of the extrusive section near Klirou bridge

We climb the slope on the south side for an overview of the northern wall of the Akaki canyon. There are three main geological units: (1) hyaloclastite breccia and thin irregular sheet flows forming the lower half of the wall are overlain by (2) 10 m thick pillows in turn overlain by (3) a thin sheet flow. The extrusives are cut by N-S striking dykes dipping steeply (70-80°) to the east and west.



Dikes intruding pillow basalt near the Klirou Bridge

Stop C1b - Close up of Klirou bridge section

Walking along the base of the cliff west of the bridge, we examine cross-cutting relationships between several generations of dykes. Sheared vesicles at the glassy margins of dykes may indicate the direction of magma flow in dyke.

Stop C2 - Volcanology of Kamara Potamos

The canyon of Kamara Potamos is about 300 m long and runs roughly E-W from the western edge of the village of Malounda, on top of the terrace, to the Akaki river.

A - Overview of northern wall of the southern branch

From our observation point below the eucalyptus grove we look at the northern wall that consists of four sheet flows, only the top of the lowermost one being exposed. The sheet flows are cut by two NNW/SSE striking normal faults, each with displacement to the west of <2m. Sheet flows thicken against the fault on the downthrown block. A 1 m thick dyke, dipping 70° to E is cut by a younger 30 cm thick sill, striking similarly but dipping up to 40°W. Where it crosses the dyke, it turns into a sill and continues eastward just above the collonade of the uppermost flow.

B - Close up of the northern wall

The fault to the right of the thick collonade is a 1m wide fracture filled with breccia, the sill cutting through the breccia.

Stop C3- Mitsero sulphide ore bodies.

Stop C4 - Field relations between lavas, umbers and radiolarites

A Theotokos Monastery to Kambia sulphide pit – a walk along the ancient ocean-floor

The Theotokos monastery stands on Maastrichtian chalk covering Turonian deep sea sediments and lavas. We inspect field relations at a brown-colored exposure on a hill 'jutting out' of the low-lying cultivated terraces. The top of the hill is built of hard brown horizon of silicified umber. Umbers are bedded, highly porous (and thus silicified) iron-manganese oxide sediments, possibly representing fallout from a black smoker plume.

At the brown hill umbers overlie basalts, but are also faulted against pink radiolarian chert – the Perapedhi formation that slowly accumulated for ~20 my while the ophiolite was under the CCD.

Stop C5 - Kambia massive sulfide deposit.

Kambia is one of more than 30 massive sulfide deposits that occur within the Troodos ophiolite, mined both for copper and, during the 1950s, for sulfur from the pyrite in them. The sulfide deposits and the underlying stockworks are similar to black smoker deposits, for example the TAG hydrothermal field in the Mid-Atlantic Ridge.

The Kambia pit exposes the stockwork pile of altered lavas intruded by veins of sulfide and quartz, ochre – the colorful weathering and oxidation products of the sulfides and the overlying unaltered lavas. A fault scar covered by debris flow of basalt pebbles cemented by jasper suggests that hydrothermal solutions flowed along fault planes to feed the seafloor springs.

Stop C6 - Volcanism in the upper lavas of the Troodos ophiolite: Margi area

A - A picrite mass 500 m SW of Margi

First considered a volcanic plug, the apparent columnar jointing of the picrite mass implies formation as part of a massive flow. However, beneath the main topographic high the picrite is intrusive into olivine basalt pillows, indicating that this is a volcanic center with a transition from a conduit into an extrusive massive flow.

B - A feeder dyke

A circular feeder pipe with a prominent chilled margin intrudes olivine basalts. The conduit has a concentric zonation passing from the chilled margin to a coarser-grained mantle of olivine basalt and then to a core of dark picrite. This suggests flow differentiation process during the ascent of magma to the surface, giving rise to pre-eruptive concentration of olivine in the liquid and providing explanation for the occurrence of picrite flows in Margi.

Day 4 - Western Limassol Forest Complex

Aims: (a) To investigate an area of the Limassol Forest that shows a very different set of features from that seen north of the Arakapas fault zone (b) To see outcrops of a low-angle detachment fault separating hanging wall sheeted dykes from footwall serpentinite. (c) To examine late igneous bodies (dykes and plutons) intruding both the footwall serpentinite and the hanging wall blocks. (d) To investigate the evolution of the deformation of the footwall serpentinite.

This field day is an essentially north-south transect through the structures and lithologies of the west end of the Limassol Forest.

Stop D1

Drive from Agros through the village of Kalokhorio. Stop at a road cut about 3 km to the west of Arakapas.

This stop is within the Arakapas Fault Zone. The fault occupies an east-west topographic trough, just as it did on the sea floor, though of course not as deep as it was then. There are few exposures of the basement of the fault zone, which is made up of deformed and metamorphosed sheeted dykes. Above this basement is a fill of clastic sediments and lavas. The clastic sediments here are breccias of sheeted dykes and lavas shed from the walls of the transform trough. Interbedded with these are lava flows of boninitic affinity. No serpentinite clasts have been reported from the breccias, so serpentinite cannot have been exposed nearby at the sea floor at the time the trough was being filled to this horizon. In contrast, on the southern edge of the western Limassol Forest, fragments of serpentinite can be seen in sediment between lava flows, showing that close to there serpentinite was already exposed at the sea floor while magmatism was still in progress.

Stop D2

Drive through the village of Arakapas southwards towards Akrounta in the southern Limassol Forest to a parking place at by a serpentinite shear zone. Walk down the road for about 500m to a high roadcut showing dykes intruding serpentinite.

A At this locality the relations between the grey dykes and purple serpentinitized harzburgite are clear. Close to the road the serpentinite contains a small intrusion of gabbro. This has been altered to rodingite, a rock made up of the calcium-aluminium minerals prehnite, pectolite and hydrogarnet. Alteration of this type shows that the gabbro was altered at the same time as the harzburgite was being serpentinitized, and must have been emplaced earlier. By contrast the dykes are chilled against the serpentinite (with very sharp chilled margins) and scarcely deformed. They have been altered at greenschist facies (black smoker) temperatures, but after most of the serpentinitization was complete. The dykes strike NE-SW, a similar orientation to the sheeted dykes north of the Arakapas Fault zone. The dykes are truncated by a late, low-angle fault about half way up the outcrop. The dykes must have been intruded into the serpentinite when it was still warm, but nearly completely serpentinitized.

B Walk back up the road to the parking place. Along the way are more dykes

intruding serpentinite. One or two of them are brown rather than grey. This indicates that they were not metamorphosed, and must have been intruded after serpentinitization was complete. The serpentinite becomes increasingly deformed by a near-vertical east-west sheared fabric. The grey dykes have been deformed by this shearing.

Stop D3

Just south of the parking area take a close look at this serpentinite shear zone in the road cut. This is part of a steep, E-W trending shear zone that can be traced for ~3km along strike. It is one of a number of such shear zones present in the mantle sequence of the Limassol Forest that are interpreted by Murton and MacLeod as transform fault-related structures. As is typical with deformed serpentinite, the fabric is not totally penetrative, but is deflected by lozenges (phacoids) of unshaped serpentinite. On top of the outcrop of this shear zone, it is possible to demonstrate that the sense of shear is broadly strike slip and dextral, though slickenline lineations on the surfaces of the phacoids do not show a consistent orientation. Such complexity is common in deformed serpentinite.

Stop D4

Now cross the road to see small outcrops of brown rock in the scrub. These outcrops are of coarse wehrlite, with brown olivine weathered down and pale green clinopyroxene standing proud of the weathered surface. The cleavage surfaces of the large clinopyroxene crystals show small rounded inclusions of olivine. These textures are typical igneous features; there is no sign of deformation in the rock. The brown colour of the olivine shows that at least some of it has not been serpentinitized. This body of rock is a late intrusion into the serpentinite, apparently after most of the deformation was complete.

Stop D5

Drive about another 2 km farther north along road to park by a long NW trending road cut.

This road cut and its extensions contain four stops all reached by walking along this section of road. At these stops it will be possible to examine the relations between serpentinite and overlying sheeted dykes, the nature of structures within the serpentinite and sheeted dykes, the timing of dyke intrusions into the serpentinite and sheeted dykes, and the geometry of a low angle detachment fault.

A Walk back along road from the parking place to a corner where the road bends sharply south. Examine the road cut on the inside of this bend. The serpentinite here shows a well-developed low-angle fabric. This is cut by a late dyke. Close to the bend is a good place to see veins of calcite precipitated from calcic/alkaline Lost City/Blue Pool spring waters produced during serpentinitization of peridotite.

B Walk back to the parking place and look at the section there, with a strong fabric in the serpentinite and a lens of brown material at the top of the road cut. This outcrop is not easy to unravel. Several of the oblique structures can be seen to be dykes truncated by a schistose shear zone below the brown material. There is a strong localized schistose fabric in some of the serpentinite. The brown material is a block of

sheeted dykes, so the contact zone is a large-offset extensional fault separating serpentinite from sheeted dykes.

C Walk farther NW along the road for about 200m. You will see on the left an outcrop of brown material stretching for about 100m along the road cut. This is an outcrop of sheeted dykes, as closer examination will show. Serpentinite underlies it. The contact between the two units can be traced very conveniently and dips at about 20° to the NE. If you scramble around on the slope below the road, it seems that the contact steepens in this direction.

Stop D6

At the top of the hill the road turns left, and straight ahead is a quarry turned into a parking/turning place. Walk into this area.

This area is backed by an excellent outcrop of sheeted dykes with the dykes striking east-west. These are in the hanging wall of the detachment fault. The sheeted dykes can be seen to be cut by isolated dykes running NE-SW, the same orientation as the dykes at Stop D1 above. While the sheeted dykes have been metamorphosed as sheeted dykes are over most of the ophiolite, these late dykes are brown and unmetamorphosed. The faulted relationship between the sheeted dykes and the serpentinite was established early in the tectonic history of this area. Both units were later cut by the post-serpentinisation dykes and plutons that we have been seeing along this transect. Look north from here across the valley of the Arakapas Fault Belt to the main Troodos Massif in the distance.

Stop D7

At the small church of Profitis Elias, the tectonic contact between sheeted dykes and serpentinite can be clearly seen, and is close to horizontal. A key stop that demonstrates the flat detachment fault.

Stop D8

Drive back up to main road and then west through Lageia (Layia) to the road cut just to the west of the village.

This classic locality preserves a >30 m thick, east-dipping section of ocean-floor sediments that were deposited onto faulted igneous basement within the Arakapas Fault Belt. The lowest part of the sequence is composed of massive units of coarse, poorly-sorted sedimentary breccia. Clasts range in size from centimetres to metres. They are dominated by blocks of lava, with some dyke rock, very rare microgabbro, and clasts of pre-existing clastic sediment. Two prominent flat rafts of finer grained clastic sediment that occur within the coarser breccias display grading that fines downwards, and may therefore be megaclasts that were turned upside down when they were incorporated into the breccia deposit. The main breccia horizon passes up into repeated fining-upward sequences of grey grits and sands alternating with fine redpurple mudstones. These are in turn overlain by a brown lava flow or sill.

Sedimentary sections such as this within the Arakapas Fault Belt are highly localised and variable. The coarse breccias are debris flow deposits, almost certainly derived from nearby fault scarps within the transform valley. The finer units are turbidites, and the red mudstone layers probably ferromanganoan sediments deposited between and/or caught up by turbidite flows. That a lava flow was extruded on top of these sediments neatly

demonstrates the ocean-floor origin of the sedimentation. The absence of serpentinite or coarse-grained gabbro or ultramafic cumulate clasts here, or anywhere else in the Arakapas Fault Belt, shows that the relief in the transform valley was not sufficient to expose deep levels of the crust or lithospheric mantle on the seafloor here. One sole outcrop of sedimentary breccia in the very south of the Limassol Forest (near Akrounda) does contain serpentinite clasts.

Day 5 - The mantle section in Mt. Olympos & a visit in the active sulfide mine in Skouriotissa

Stop E1 – This stop is a walk in the circum trails around the summit of Mt. Olympos, Atalante and Artemis, with a spectacular scenery over Cyprus. In these trails we will walk through a province of dunites (see Glossary) and harzburgites, and pegmatitic gabbro dike intruding into the mantle sequence. We will discuss the mode of melt transport through the mantle towards the axial oceanic crust. We will also see joints filled with serpentinites and pyroxenites.



Pegmatitic gabbro intruding dunite at the Atalante trail

Stop E2 – A visit in the active mine of massive sulfide deposits of Skouriotissa.



Massive sulfide deposits in Skouriotissa mine

References

- Abelson, M., G. Baer, and A. Agnon Evidence from gabbro of the Troodos Ophiolite for lateral magma transport along a slow-spreading mid-ocean ridge, *Nature (London)* (2001), 409(6816):72-75
- Abelson, M., G. Baer, and A. Agnon (2002), Fossil ridge-transform intersection in the Troodos ophiolite: new perspectives from rock magnetism in the gabbro suite and fracture mechanics analysis, *Geochem. Geophys. Geosyst.*, 3(8), doi: 10.1029/2004JB003473.
- Allerton, S and Vine F.J., 1990. Palaeomagnetic and structural studies of the southeastern part of the Troodos Complex. In: *Ophiolites; oceanic crustal analogues* (eds. Malpas, J., Moores, E.M., Panayiotou, A. & Xenophontos, C.) Geological Survey Department, Nicosia, Cyprus. pp 99-111.
- Bonhommet, N., Roperch, P. & Calza, F. 1988. Paleomagnetic arguments for block rotations along the Arakapas fault (Cyprus) *Geology* **16**, 422-425.
- Cann, J.R., H. M. Prichard, J. G. Malpas, and C. Xenophontos, Oceanic inside corner detachments of the Limassol Forest area, Troodos Ophiolite, Cyprus, *Journal of the Geological Society of London* (2001), 158, Part 5 757-767
- Cann, J.R., McCaig, A., MacLeod, C. J., Field Trip Guide, AGU Chapman Conference - Detachments in oceanic lithosphere: Deformation, magmatism, fluid flow, and ecosystems. Agros, Cyprus, May 2010.
- Gass, I.G. 1968, Is the Troodos Massif of Cyprus a fragment of Mesozoic ocean floor? *Nature*, 220, 39-42.
- Gass, I.G., MacLeod, C.J., Murton, B.J., Panayiotou, A., Simonian, K.O. & Xenophontos, C. 1994 The geology of the Southern Troodos Transform Zone. Memoir 9, Geological Survey Department, Nicosia, Cyprus.
- Gillis, K.M. and P.T. Robinson, Patterns and processes of alteration in the lavas and dykes of the Troodos Ophiolite, Cyprus, *J. Geophys. Res.*, 95, 21,523-21,548, 1990.
- Gillis, K. M. and L. A. Coogan, Anatectic migmatites from the roof of an ocean ridge magma chamber, *Journal of Petrology* (2002), 43(11):2075-2095
- Hurst, S.D., Moores, E.M. & Varga, R.J. Structural and geophysical expression of the Solea Graben, Troodos ophiolite, Cyprus. *Tectonics*, 13, 139-156, 1994
- Kelley, D.S. & Malpas, J.G. Processes of brine generation and circulation in the oceanic crust: fluid inclusion evidence from the Troodos ophiolite, Cyprus. *J. Geophys. Res.* 97, 307-322, 1992
- Kidd, R.G.W., and Cann, J.R., 1974, Chilling statistics indicate an ocean-floor spreading origin for the Troodos complex, Cyprus: *Earth and Planetary Science Letters*, v. 24, p. 151-155.
- Malpas, J., Xenophontos, C., and Cann, J., Field trip guide, The Troodos Ophiolite, The 3rd International Conference on the Geology of the Eastern Mediterranean, Nicosia, Cyprus, 1998.
- Malpas, J., 1990, Crustal accretionary processes in the Troodos Ophiolite, Cyprus; evidence from field mapping and deep crustal drilling, in Malpas, J., Moores, E.M., Panayiotou, A., and Xenophontos, C., eds., *Ophiolites; oceanic crustal analogues; proceedings of the symposium "Troodos 1987"*, Nicosia, Cyprus, *Minist. Agric. and Nat. Resour.*, p. 65-74.
- MacLeod, C.J. and Murton, B.J. 1993 Structure and tectonic evolution of the Southern Troodos Transform Fault Zone, Cyprus In: Prichard, H.M., Alabaster, T., Harris, N.B.W. and Neary, C.R. eds. *Magmatic processes and plate tectonics*, Geological Society Special Publication no 76, pp 141-176
- Moores, E.M. & Vine, F.J., 1971. The Troodos massif, Cyprus, and other ophiolites as oceanic crust: evaluation and implications. *Phil. Trans. R. Soc. Lond.* A268, 443-466.
- Morris, A., Creer, K.M. & Robertson, A.H.F., 1990. Palaeomagnetic evidence for clockwise rotations related to dextral shear along the Southern Troodos Transform Fault, Cyprus. *Earth Planet. Sci. Lett.*, **99**, 250-262.
- Nuriel, P., Y.Katzir, M.Abelson, J.W.Valley, A.Matthews, M.J.Spicuzza and A.Ayalon, 2009. Faultrelated oceanic serpentinization in the Troodos ophiolite, Cyprus: implications for a fossil oceanic core complex. *Earth and Planet. Sci. Lett.*, 282, 34-46.
- Pearce, J.A., 2003, *Supra-subduction zone ophiolites; the search for modern analogues* GSA SP 373 pp. 269-293.
- Schmincke, H.-U. & Bednarz, U. Pillow, sheet flows and breccia flow volcanoes and volcano-tectonic hydrothermal cycles in the extrusive series of the northeastern Troodos ophiolite, Cyprus. In: *Ophiolites; oceanic crustal analogues* (eds. Malpas, J., Moores, E.M., Panayiotou, A. & Xenophontos, C.) Geological Survey Department, Nicosia, Cyprus. pp 207-216, 1990
- Simonian, K.O. and Gass, I.G. 1978. Arakapas fault belt, Cyprus: a fossil transform fault. *Geol. Soc. Amer. Bull.*, 89, 1220-1230
- Richardson, C.J., J.R. Cann, H.G. Richards and J.G. Cowan, Metal-depleted root zones of the Troodos ore-forming hydrothermal systems, Cyprus, *Earth Planet. Sci. Lett.*, 84, 243-253, 1987.
- Robertson, A.H.F., Clift, P.D., Degnan, P.J. & Jones, G., 1991, Palaeoceanographic and palaeotectonic evolution of the Eastern Mediterranean Neotethys. *Paleogeog. Palaeoclim. Palaeocol.* 87, 289-343.

- Staudigel, Hubert, L. Tauxe, J. S. Gee, P. Bogaard, J. Haspels, G. Kale, A. Leenders, P. Meijer, B. Swaak, M. Tuin, M. C. VanSoest, E. A. T. Verdurmen, and A. Zevenhuizen, Geochemistry and intrusive directions in sheeted dikes in the Troodos Ophiolite; implications for mid-ocean ridge spreading centers, *Geochemistry, Geophysics, Geosystems* (1999), 1
- Varga, R.J. Modes of extension at oceanic spreading centres: evidence from the Solea Graben, Troodos ophiolite, Cyprus. *J. Struct. Geol.* 13, 517-537, 1991
- Varga, R. J., Gee, J. S., Bettison-Varga, L., Anderson, R. S., and Johnson, C. L., 1999, Early establishment of seafloor hydrothermal systems during structural extension: paleomagnetic evidence from the Troodos Ophiolite: *Earth and Planetary Science Letters*, v. 171, p. 221-235.

A useful glossary for Troodos field trip

Boninite is a mafic extrusive rock high in both magnesium and silica, formed in fore-arc environments, typically during the early stages of subduction. The rock is named for its occurrence in the Izu-Bonin arc south of Japan. It is characterized by extreme depletion in incompatible trace elements that are not fluid mobile (e.g., the heavy rare earth elements plus Nb, Ta, Hf) but variable enrichment in the fluid mobile elements (e.g., Rb, Ba, K). They are found almost exclusively in the fore-arc of primitive island arcs (that is, closer to the trench) and in ophiolite complexes thought to represent former fore-arc settings. Boninite is considered to be a *primitive* andesite derived from melting of metasomatised mantle.

Diabase (pronounced /ˈdaɪ.əbeɪs/) or **dolerite** is a mafic, holocrystalline, subvolcanic rock equivalent to volcanic basalt or plutonic gabbro. In North American usage, the term *diabase* refers to the fresh rock, whilst elsewhere the term *dolerite* is used for the fresh rock and *diabase* refers to altered material.^{[1][2]} Diabase dikes and sills are typically shallow intrusive bodies and often exhibit fine grained to aphanitic chilled margins which may contain tachylite (dark mafic glass). Diabase normally has a fine, but visible texture of euhedral lath-shaped plagioclase crystals (62%) set in a finer matrix of clinopyroxene, typically augite (20–29%), with minor olivine (3% up to 12% in olivine diabase), magnetite (2%), and ilmenite (2%).^[3] Accessory and alteration minerals include hornblende, biotite, apatite, pyrrhotite, chalcopyrite, serpentine, chlorite, and calcite.

Gabbro (■ /ˈɡæbrɔʊ/) refers to a large group of dark, coarse-grained, intrusive mafic igneous rocks chemically equivalent to basalt. The rocks are plutonic, formed when molten magma is trapped beneath the Earth's surface and cools into a crystalline mass. The vast majority of the Earth's surface is underlain by gabbro within the oceanic crust, produced by basalt magmatism at mid-ocean ridges.

Gabbro is dense, greenish or dark-colored and contains pyroxene, plagioclase, amphibole, and olivine (olivine gabbro when olivine is present in a large amount). The pyroxene is mostly clinopyroxene; small amounts of orthopyroxene may be present. If the amount of orthopyroxene is substantially greater than the amount of clinopyroxene, the rock is then a **norite**. Gabbros contain minor amounts, typically a few percent, of iron-titanium oxides such as magnetite, ilmenite, and ulvospinel.

Gabbro is generally coarse grained, with crystals in the size range of 1 mm or greater. Finer grained equivalents of gabbro are called diabase, although the vernacular term *microgabbro* is often used when extra descriptiveness is desired. Gabbro may be extremely coarse grained to pegmatitic, and some pyroxene-plagioclase cumulates are essentially coarse grained gabbro, although these may exhibit acicular crystal habits. Gabbro is usually equigranular in texture, although it may be porphyritic at times, especially when plagioclase oikocrysts have grown earlier than the groundmass minerals.

Hyaloclastite is a hydrated tuff-like breccia rich in black volcanic glass, formed during volcanic eruptions under water, under ice or where subaerial flows reach the sea or other bodies of water. It has the appearance of angular flat fragments sized between a millimeter to few centimeters. The fragmentation occurs by the force of the volcanic explosion, or by thermal shock during rapid cooling. Several minerals are found in hyaloclastite masses. Sideromelane is a basalt glass rapidly quenched in water. It is transparent and pure, lacking the iron oxide crystals dispersed in the more commonly occurring tachylite. Fragments of these glasses are usually surrounded by a yellow waxy layer of palagonite, formed by reaction of sideromelane with water. Hyaloclastite ridges, formed by subglacial eruptions during the last glacial period, are a prominent landscape feature of Iceland and British Columbia. Hyaloclastite is usually found at

subglacial volcanoes, such as tuyas, which is type of distinctive, flat-topped, steep-sided volcano formed when lava erupts through a thick glacier or ice sheet.

A **hydrothermal vent** is a fissure in a planet's surface from which geothermally heated water issues. Hydrothermal vents are commonly found near volcanically active places, areas where tectonic plates are moving apart, ocean basins, and hotspots. Hydrothermal vents exist because the earth is both geologically active and has large amounts of water on its surface and within its crust. Common land types include hot springs, fumaroles and geysers. Under the sea, hydrothermal vents may form features called *black smokers*. Relative to the majority of the deep sea, the areas around submarine hydrothermal vents are biologically more productive, often hosting complex communities fueled by the chemicals dissolved in the vent fluids.

Hydrothermal vents in the deep ocean typically form along the Mid-ocean ridges. The water that issues from seafloor hydrothermal vents consists mostly of sea water drawn into the hydrothermal system close to the volcanic edifice through faults and porous sediments or volcanic strata, plus some magmatic water released by the upwelling magma

A *black smoker* or *sea vent* is a type of hydrothermal vent found on the seabed, typically in the abyssal and hadal zones. They appear as black chimney-like structures that emit a cloud of black material. The black smokers typically emit particles with high levels of sulfur-bearing minerals, or sulfides. Black smokers are formed in fields hundreds of meters wide when superheated water from below Earth's crust comes through the ocean floor. This water is rich in dissolved minerals from the crust, most notably sulfides. When it comes in contact with cold ocean water, many minerals precipitate, forming a black chimney-like structure around each vent. The metal sulfides that are deposited can become massive sulfide ore deposits in time. Black smokers were first discovered in 1977 on the East Pacific Rise by scientists from Scripps Institution of Oceanography. They were observed using a deep submergence vehicle called Alvin belonging to the Woods Hole Oceanographic Institution. Now black smokers are known to exist in the Atlantic and Pacific Oceans, at an average depth of 2100 metres. The most northerly black smokers are a cluster of five named Loki's Castle,^[7] discovered in 2008 by scientists from the University of Bergen at 73 degrees north, on the Mid-Atlantic Ridge between Greenland and Norway.

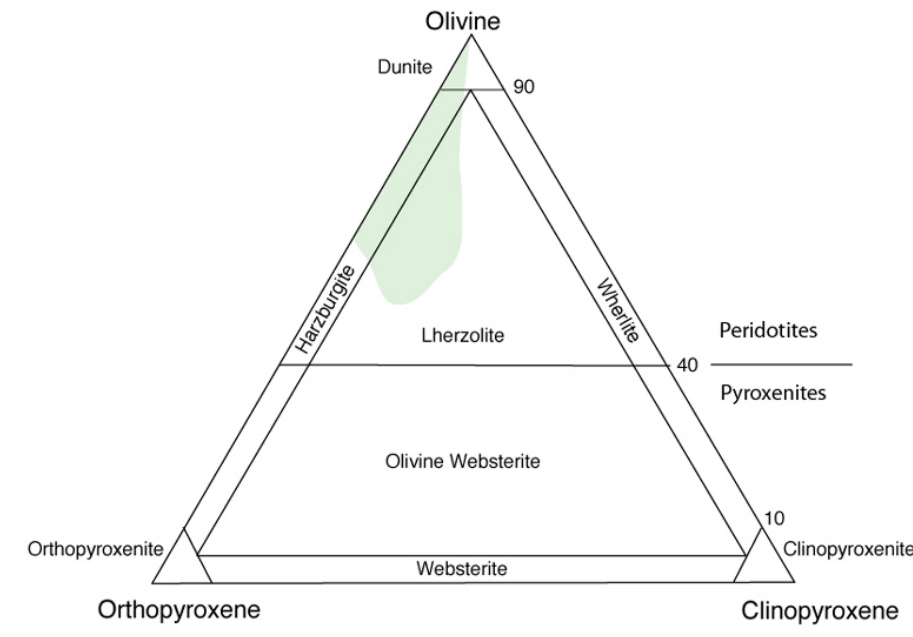
Jasper, a form of chalcedony,^[1] is an opaque,^[2] impure variety of silica, usually red, yellow, brown or green in color; and rarely blue. This mineral breaks with a smooth surface, and is used for ornamentation or as a gemstone. It can be highly polished and is used for vases, seals, and at one time for snuff boxes. Jasper is basically chert which owes its red color to iron(III) inclusions. The specific gravity of jasper is typically 2.5 to 2.9.^[3] The jasper was a stone in the Jewish High Priest's breastplate, described in Exodus 28. The name means "spotted or speckled stone", and is derived via Old French *jaspre* (variant of Anglo-Norman *jaspe*) and Latin *iaspidem* (nom. *iaspis*) from Greek ἰασπίς *iaspis*, (feminine noun)^[4] from a Semitic language (cf. Hebrew יִשְׁפָּה *yushphah*, Akkadian *yashupu*), ultimately from Persian یاشپ *yašp*.^[5] Jasper is an opaque rock of virtually any color stemming from the mineral content of the original sediments or ash. Patterns arise during the consolidation process forming flow and depositional patterns in the original silica rich sediment or volcanic ash. Hydrothermal circulation is generally thought to be required in the formation of jasper.

The **Messinian** is in the geologic timescale the last age or uppermost stage of the Miocene. It spans the time between 7.246 ± 0.005 Ma and 5.332 ± 0.005 Ma (million years ago). It follows the Tortonian and is followed by the Zanclean, the first age of the Pliocene. The Messinian overlaps the Turolian European Land Mammal Mega Zone (more precise MN 12 and 13) and the Pontian Central European Paratethys stage. It also overlaps the late Huayquerian and early Montehermosan South American Land Mammal Ages, and falls inside the more extensive Hemphillian North American Land Mammal Age. During the Messinian, around 6 million years ago, the Messinian salinity crisis took place, which brought about repeated desiccations of the Mediterranean Sea.

A **peridotite** is a dense, coarse-grained igneous rock, consisting mostly of the minerals olivine and pyroxene. Peridotite is ultramafic, as the rock contains less than 45% silica. It is high in magnesium, reflecting the high proportions of magnesium-rich olivine, with appreciable iron. Peridotite is derived from the Earth's mantle, either as solid blocks and fragments, or as crystals accumulated from magmas that formed in the mantle. The compositions of peridotites from these layered igneous complexes vary widely, reflecting the relative proportions of pyroxenes, chromite, plagioclase, and amphibole.

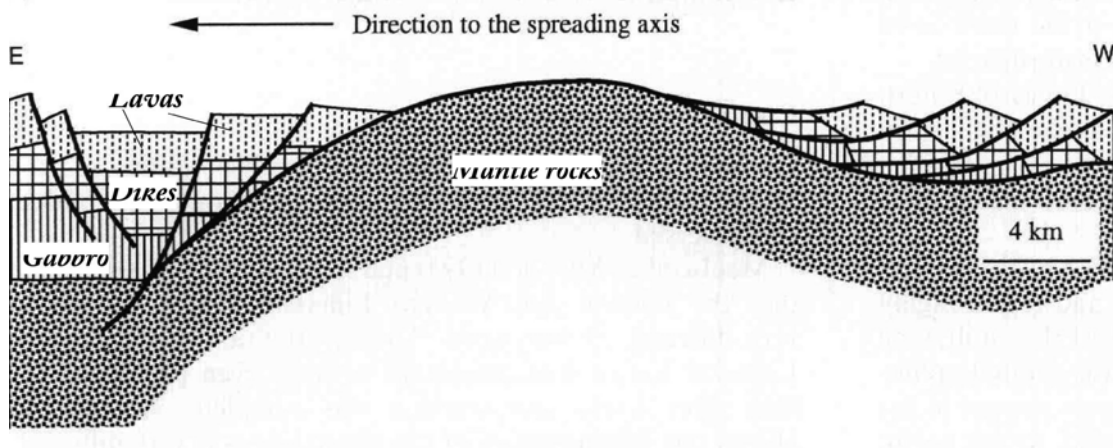
Types of peridotite

- Dunite: more than 90% olivine, typically with Mg/Fe ratio of about 9:1.
- Wehrlite: mostly composed of olivine plus clinopyroxene.
- Harzburgite: mostly composed of olivine plus orthopyroxene, and relatively low proportions of basaltic ingredients (because garnet and clinopyroxene are minor).
- Lherzolite: mostly composed of olivine, orthopyroxene (commonly enstatite), and clinopyroxene (diopside), and have relatively high proportions of basaltic ingredients (garnet and clinopyroxene). Partial fusion of lherzolite and extraction of the melt fraction can leave a solid residue of harzburgite.



An **oceanic core complex (OCC)**, or **megamullion**, is a seabed geologic feature that forms a long ridge perpendicular to a mid-ocean ridge. It contains smooth domes that are lined with transverse ridges like a corrugated roof. They can vary in size from 10 to 150 km in length, 5 to 15 km in width, and 500 to 1500 m in height. The first oceanic core complexes described were identified in the Atlantic Ocean (Cann et al., 1998; Tucholke et al., 1998). Since then numerous such structures have been identified primarily in oceanic lithosphere formed at intermediate, slow- and ultra-slow spreading mid-ocean ridges, as well as back-arc basins (Fujimoto et al., 1999; O'Hara et al., 2001). Examples include large expanses of ocean floor and therefore of the oceanic lithosphere, particularly along the Mid-Atlantic Ridge (Smith et al., 2006; Escartin et al., 2008) and the Southwest Indian Ridge (Cannat et al., 2006). Some of these structures have been drilled and sampled, showing that the footwall can be composed of both mafic plutonic and ultramafic rocks (gabbro and peridotite primarily, in addition to diabase), and a thin shear zone that includes hydrous phyllosilicates. Oceanic core complexes are often associated with active hydrothermal fields. Oceanic core complex structures form at slow spreading oceanic plate

boundaries which have a limited supply of upwelling magma. These zones have low upper mantle temperatures and long transform faults develop. Rift valleys do not develop along the expansion axes of slow spreading boundaries. Expansion takes place along low-angle detachment faults. The core complex builds on the upper block of the fault where most of the gabbroic (or crustal) material is stripped away to expose mantle peridotite. They comprise peridotites ultramafic rocks of mantle and to a lesser extent gabbroic rocks from the Earth's crust. Each detachment fault has three notable features: a breakaway zone where the fault began, an exposed fault surface that rides over the dome and a termination, which is usually marked by a valley and adjacent ridge.



Ochre or **ocher** (pronounced /'oʊkər/ OH-kər, from the Greek ὄχρος, *ōkhrós*, pale) is the term for both a golden-yellow or light yellow brown-- color and for a form of earth pigment which produces the color. Ochres are among the earliest pigments used by mankind, derived from naturally tinted clay containing mineral oxides. Chemically, it is hydrated iron (III) oxide.

As a painting pigment, it exists in at least four forms:

- **Yellow ochre**, $\text{Fe}_2\text{O}_3 \cdot \text{H}_2\text{O}$, a hydrated iron oxide, also called **Gold ochre**
- **Red ochre**, Fe_2O_3 , the anhydrate of yellow ochre, which turns red when heated, as this drives off the water ligands.
- **Purple ochre**, identical to red ochre chemically but of a different hue caused by different light diffraction properties associated with a greater average particle size
- **Brown ochre** (Goethite), also partly hydrated iron oxide (rust)

Picrite basalt, **picrobasalt** or **oceanite**^[citation needed] is a variety of high-magnesium olivine basalt that is very rich in the mineral olivine. It is dark with yellow-green olivine phenocrysts (20 to 50%) and black to dark brown pyroxene, mostly augite. The olivine-rich picrite basalts that occur with the more common tholeiitic basalts of Kīlauea and other volcanoes of the Hawaiian Islands are the result of accumulation of olivine crystals either in a portion of the magma chamber or in a caldera lava lake.^[1] The compositions of these rocks are well-represented by mixes of olivine and more typical tholeiitic basalt. The name "picrite" can also be applied to an olivine-rich alkali basalt: such picrite consists largely of phenocrysts of olivine and titanium-rich augite pyroxene with minor plagioclase set in a groundmass of augite and more sodic plagioclase and perhaps analcite and biotite. Picrites and komatiites are somewhat similar chemically, but differ in that komatiite lavas are products of more magnesium-rich melts, and good examples exhibit the spinifex texture.^[2] In contrast, picrites are magnesium-rich because crystals of olivine have accumulated in more normal melts by magmatic processes. Komatiites are largely restricted to the Archean. When the term *oceanite* was apparently first proposed by Lacroix, he used the term to apply only to basalts with more than 50% olivine content (an extremely rare occurrence). Picrite

basalt is found in the lavas of Mauna Kea and Mauna Loa in Hawai‘i^[3], Curaçao, in the Piton de la Fournaise^[4] volcano on Réunion Island and various other oceanic island volcanoes. Picrite basalt has been erupted in historical times from Mauna Loa during the eruptions of 1852 and 1868 (from different flanks of Mauna Loa)^[5]. Picrite basalt with 30% olivine commonly erupts from the Piton de la Fournaise. [6]

Seafloor massive sulfide deposits or SMS deposits, are modern equivalents of ancient volcanogenic massive sulfide ore deposits or VMS deposits. The term has been coined by mineral explorers to differentiate the modern deposit from the ancient. SMS deposits were first recognised during the exploration of the deep oceans and the mid ocean ridge spreading centers in the early 1960s. Deep ocean bathyspheres and remote operated vehicles have visited and taken samples of black smoker chimneys, and it has been long recognised that such chimneys contain appreciable grades of Cu, Pb, Zn, Ag, Au and other trace metals. SMS deposits are currently forming in the deep ocean around submarine volcanic arcs, where hydrothermal vents exhale sulfide-rich mineralising fluids into the ocean. SMS deposits are laterally extensive and consist of a central vent mound around the area where the hydrothermal circulation exits, with a wide apron of unconsolidated sulfide silt or ooze which precipitates upon the seafloor.

Serpentinite is a rock composed of one or more serpentine group minerals. Minerals in this group are formed by **serpentinization**, a hydration and metamorphic transformation of ultramafic rock from the Earth's mantle. The alteration is particularly important at the sea floor at tectonic plate boundaries. Serpentinization is a geological low-temperature metamorphic process involving heat and water in which low-silica mafic and ultramafic rocks are oxidized (anaerobic oxidation of Fe²⁺ by the protons of water leading to the formation of H₂) and hydrolyzed with water into serpentinite. Peridotite, including dunite, at and near the seafloor and in mountain belts is converted to serpentine, brucite, magnetite, and other minerals — some rare, such as awaruite (Ni₃Fe), and even native iron. In the process large amounts of water are absorbed into the rock increasing the volume and destroying the structure.^[1] The density changes from 3.3 to 2.7 g/cm³ with a concurrent volume increase of about 40%. The reaction is exothermic and large amounts of heat energy are produced in the process.^[1] Rock temperatures can be raised by about 260 °C,^[1] providing an energy source for formation of non-volcanic hydrothermal vents. The magnetite-forming chemical reactions produce hydrogen gas under anaerobic conditions prevailing deep in the mantle, far from the Earth atmosphere. Carbonates and sulfates are subsequently reduced by hydrogen and form methane and hydrogen sulfide. The hydrogen, methane, and hydrogen sulfide provide energy sources for deep sea chemotroph microorganisms.^[1] Serpentinite is formed from olivine via several reactions, some of which are complementary. Olivine is a solid solution between the magnesium-endmember forsterite and the iron-endmember fayalite. Serpentinite reactions 1a and 1b, below, exchange silica between forsterite and fayalite to form serpentine group minerals and magnetite. These are highly exothermic reactions.

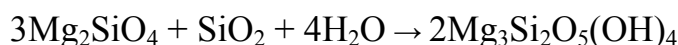
Reaction 1a:

Fayalite + water → magnetite + aqueous silica + hydrogen



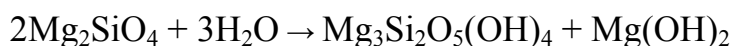
Reaction 1b:

Forsterite + aqueous silica → serpentine



Reaction 1c:

Forsterite + water → serpentine + brucite



Reaction 1c describes the hydration of olivine with water only to yield serpentine and Mg(OH)₂ (brucite). Serpentine is stable at high pH in the presence of brucite like calcium silicate hydrate,

(C-S-H) phases formed along with portlandite ($\text{Ca}(\text{OH})_2$) in hardened Portland cement paste after the hydration of belite (Ca_2SiO_4), the artificial calcium equivalent of forsterite.

Tremolite is a member of the amphibole group of silicate minerals with composition: $\text{Ca}_2\text{Mg}_5\text{Si}_8\text{O}_{22}(\text{OH})_2$. Tremolite forms by metamorphism of sediments rich in dolomite and quartz. Tremolite forms a series with actinolite and ferro-actinolite. Pure magnesium tremolite is creamy white, but the color grades to dark green with increasing iron content. It has a hardness on Mohs scale of 5 to 6. Nephrite, one of the two minerals of the gemstone jade, is a green variety of tremolite. A fibrous variety of tremolite is used as asbestos. This material is toxic and inhaling the fibers can lead to asbestosis, lung cancer and mesothelioma. Tremolite is an indicator of metamorphic grade since at high temperatures it converts to diopside. Calcite, grossular, talc, and serpentine are common associates of tremolite. Tremolite is also found on top of masifs of oceanic core-complexes. The surface of this massif is a fault zone composed of talc-tremolite-chlorite schists, metamorphosed at greenschist facies (black smoker temperatures), with a footwall composed of serpentinized peridotites intruded by gabbro bodies (Escartín et al., 2003). The schists are of predominantly ultramafic protolith, as shown by trace element contents and the presence of relict chromite grains.

Trondhjemite is a leucocratic (light-colored) intrusive igneous rock. It is a variety of tonalite in which the plagioclase is mostly in the form of oligoclase. Trondhjemites are sometimes known as **plagiogranites**. Trondhjemite is common in Archean terranes occurring in conjunction with tonalite and granodiorite as the *TTG* (tonalite-trondhjemite-granodiorite) orthogneiss suite. Trondhjemite dikes also commonly form part of the sheeted dike complex of an ophiolite.

Umbra is an iron and manganese-rich **hydrothermal sediments**. These sediments are interpreted as fallout from black smoker plumes, formed by oxidation of the iron sulphide black smoke particles in the water column and by adsorption of hydrothermal manganese from the diluted hydrothermal solutions onto the newly formed iron oxides. They subsequently accumulated on the seafloor and were preserved in hollows in the seabed. The name derives from the Latin word *umbra* (shadow) and was originally extracted in Umbria, a mountainous region of central Italy,^[1] but it is found in many parts of the world. Chemical formula: $\text{Fe}_2\text{O}_3 + \text{MnO}_2 + \text{H}_2\text{O} + \text{Si} + \text{Al}_2\text{O}_3$

Discovery of “Megamullions” Reveals Gateways Into the Ocean Crust and Upper Mantle

Brian E. Tucholke

Senior Scientist, Geology & Geophysics Department

Long before the plate-tectonic revolution began in the 1960s, scientists envisioned drilling into the ocean crust to investigate Earth’s evolution. As early as 1881, Darwin suggested drilling Pacific atolls for scientific purposes. From the end of the nineteenth into the first half of the twentieth century, drilling was used to penetrate the reef and uppermost volcanic foundation of several oceanic islands, and these glimpses of oceanic geology whetted the scientific community’s appetite for deeper and more complete data.

The idea of ocean drilling gained momentum in the 1950s and resulted in the “Mohole project,”

whose objective was to sample the material beneath the Mohorovicic discontinuity, or “Moho,” the boundary between Earth’s crust and mantle. The Mohole project proved to be ahead of its time, but the program’s test drilling in the deep eastern Pacific Ocean proved that ocean crust could be successfully drilled and cored from a dynamically positioned ship in several thousand meters of water. Mohole was succeeded beginning in the late 1960s by the hugely successful Deep Sea Drilling Project, the International Phase of Ocean Drilling, and the current Ocean Drilling Program. (For “An Abridged History of Deep Ocean Drilling” by Arthur E. Maxwell, see *Oceanus* Vol. 36, No. 4.)

A major scientific goal of all these efforts has been to recover a complete section of normal ocean crust and uppermost mantle. The lithology, properties,

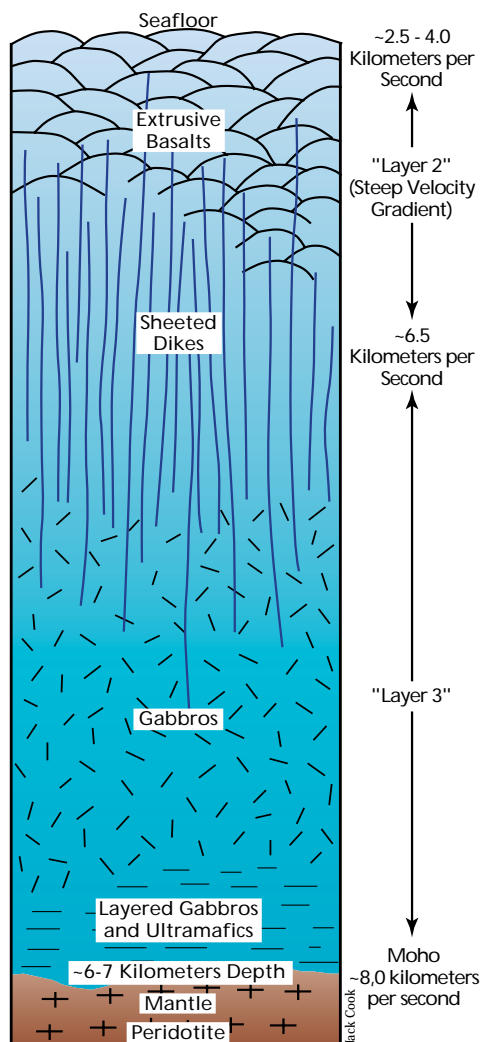
and geological relations of these rocks are key to understanding such varied phenomena as convection in the earth’s mantle, melting and transport mechanisms in the upwelling asthenosphere beneath mid-ocean ridges, rock deformation and alteration, the sources of magnetic anomalies in ocean basins, and hydrothermal circulation and formation of ore deposits.

Poking at the Oceanic Lithosphere

The outstanding obstacle to drilling through the entire ocean crust is that normal crustal thickness is on the order of 6 to 7 kilometers. Penetrating it

beneath several thousand meters of water is presently at the limits of drilling technology as well as beyond the financial boundaries of scientific funding. Currently, drilling to depths of 1.5 to 2 kilometers has yielded upper ocean crust samples, as well as sections of deeper crust and upper mantle where these rocks are exposed by natural tectonic processes. Pieced together, these sections are in many ways similar to our conception of what ocean crust should look like, based on studies of ophiolites, old seafloor parcels that have been exposed above sea level by various tectonic mechanisms. (See map on page 24.)

At its base, the “standard ophiolite model” (see figure at left) includes an “ultramafic” layer (made up of dense rock rich in iron and magnesium) that represents the oceanic mantle. The overlying crust is formed from melt that rose buoy-



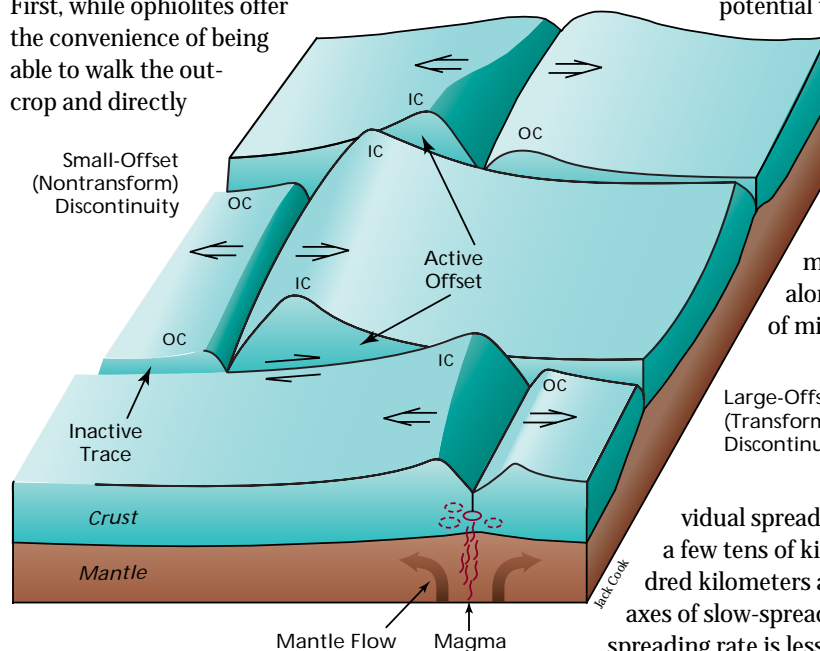
Schematic section through oceanic crust, based on study of subaerially exposed ophiolites and drilling results in the ocean basins. Boundaries between lithologic units are usually transitional and complex, and units may be thin or missing where magma input is episodic, notably on slow-spreading ridges.

antly at a mid-ocean ridge from the hot, upwelling mantle. From bottom to top, the crust consists of layers formed by crystallization in presumed magma chambers or zones of hot crystal mush, a shallower section of vertically oriented, intrusive dikes,* and a volcanic surface layer of pillow basalts extruded onto the seafloor and capped by sediments. Laboratory analyses show that each of these sequences transmits sound waves with characteristic velocities, and seismologists studying sound propagation in the deep ocean basins have roughly equated observed crustal velocity layering with rock type in the standard ophiolite model. From mapping of seismic velocities, the subseafloor depth of the top of the mantle (the Moho), and thus the apparent thickness of normal ocean crust, appears to be remarkably uniform at about 6 to 7 kilometers.

However, there are several problems with relying too heavily on the ophiolite and velocity models.

First, while ophiolites offer the convenience of being able to walk the out-crop and directly

Sketch of spreading segments separated by ridge-axis discontinuities in slow-spreading ocean crust. The crust at inside corners (IC) differs significantly from that at outside corners (OC) in that it is more elevated, thinner, and faulted into a blockier fabric. This asymmetry is thought to be caused by consistent dip of faults from inside corners to beneath outside corners, so that lower crust and upper mantle are commonly exhumed in the IC footwalls of the faults. Near a segment center on the front face of the diagram, hot, upwelling mantle decompresses and partially melts, supplying magma that is intruded and extruded to form the ocean crust.



study geological relationships, there is considerable debate as to their value for interpreting the structure of normal ocean crust. Many ophiolites are known to have originated in unusual tectonic settings such as behind island arcs or above subduction zones, and it is uncertain how representative they are of crust beneath most large ocean basins. Second, it is likely that the standard ophiolite model is overly simplistic. Spreading rates and the associated levels and constancy of magma production vary dramatically among mid-ocean ridges, so the magmatic and tectonic structure of deep ocean crust probably seldom approaches the ideal model, particularly where magma supply is limited. Finally, our suppositions about the relative uniformity of crustal thickness and composition, as inferred from velocity-lithology correlations, could be seriously in

*Dikes form when vertical fissures allow molten material to rise through preexisting structures.

error. In particular, normally high-velocity ultramafics of the upper mantle may become altered by seawater that penetrates deeply along faults and fractures. Such alteration can dramatically reduce sound velocity in these rocks, making them appear seismically to be part of the ocean crust and thus causing us to overestimate true crustal thickness.

To resolve such uncertainties, we are still faced with the need systematically to sample the entire crustal and uppermost mantle sequence within the ocean basins. To date, the best path to this goal has been to sample local tectonic exposures, but because of the intermittency and incompleteness of outcrops, this has been considered a piecemeal solution at best. Recent discoveries, however, indicate that complete, naturally occurring crust-mantle cross sections may be exposed on the seafloor by unusually long-lived faults. These sections have the

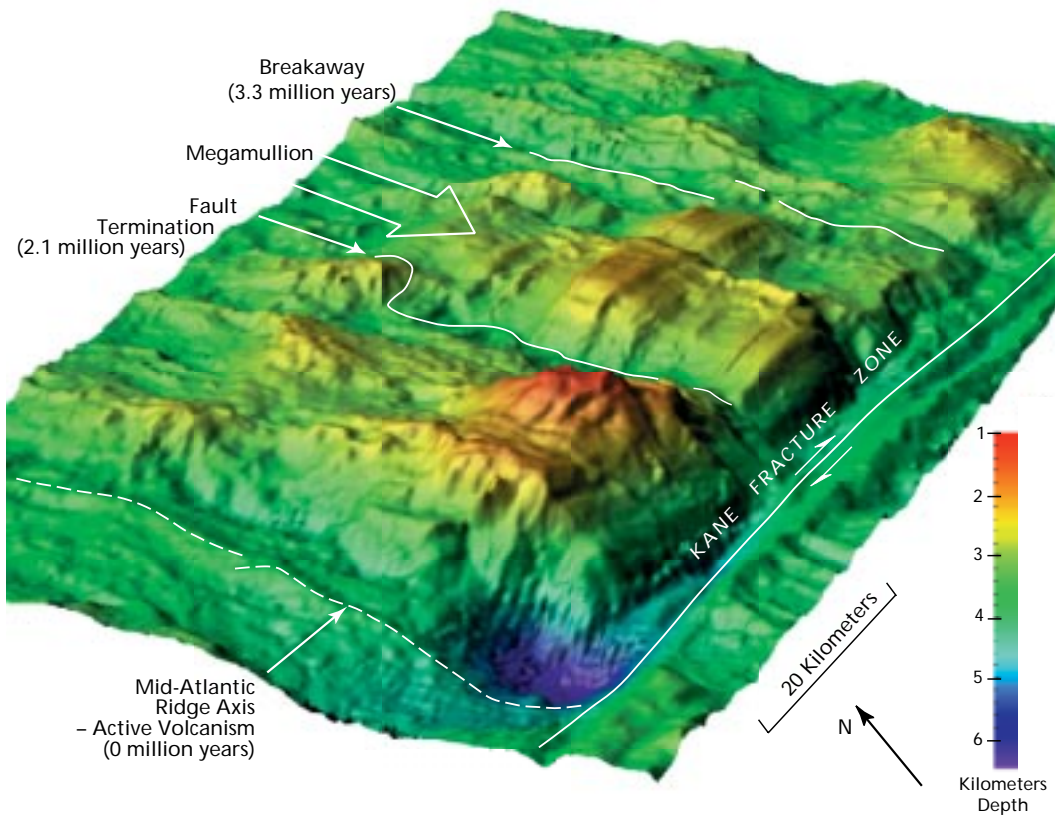
potential to yield long-sought answers to questions about the structure and origin of oceanic crust.

Nature Opens the Door

To understand how tectonism exposes cross sections of the ocean crust, we must first consider the typical along- and across-axis structure of mid-ocean ridge (see figure at left). The spreading axis, where magma wells up to form new ocean crust, is offset by discontinuities to form numerous indi-

vidual spreading segments that extend from a few tens of kilometers to more than a hundred kilometers along the ridge axis. At the axes of slow-spreading ridges (where total spreading rate is less than about 35 to 40 millimeters per year), seismic studies of spreading segments, together with gravity studies of density distribution and direct seafloor sampling by dredging and submersible, indicate that crustal thickness is greatest near segment centers and that it thins markedly toward the discontinuities at segment ends. From this, we infer that upwelling of magma from the mantle is relatively focused near the centers of slow-spreading segments. At faster-spreading ridges, in contrast, crustal thickness tends to be more uniform along the length of spreading segments, and upwelling of magma therefore appears to be more evenly distributed along a segment.

Another significant difference between slow- and fast-spreading ridges is in magma supply. The rate of magma supply at slow-spreading ridges is relatively low compared to the rate of axial crust extension, while the rates are more comparable at fast-spreading ridges. The result is that tectonic extension,

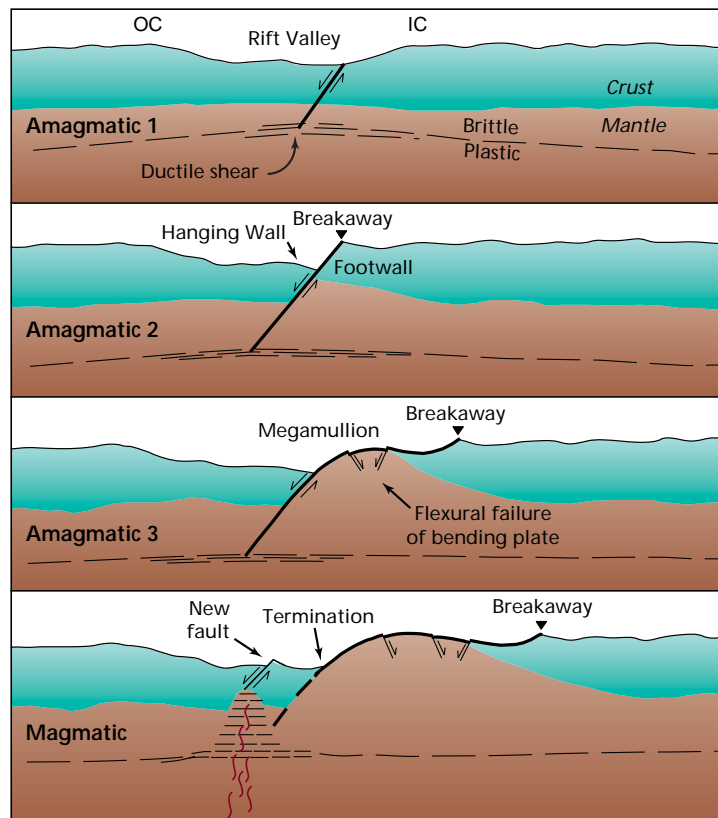


Perspective view, looking southwest, of a megamullion that developed at an inside corner of the Kane transform discontinuity between about 3.3 and 2.1 million years ago. The domed megamullion is corrugated by ridges (mullions) that parallel the direction of fault slip. A steep, west-facing normal fault formed as the megamullion developed, and it cuts the mullions at right angles. The image was generated from multibeam sonar data that give complete bathymetric coverage of the seafloor.

expressed in the form of large normal faults, is much more profound at slow-spreading ridges, particularly at segment ends. These faults cut deeply into and sometimes through the ocean crust. If extension occurs for a long enough period on a fault, then a significant portion of the ocean crustal section, and possibly even upper-mantle rocks, could be exhumed along the fault plane. Do these geological cross sections actually exist on the seafloor, and, if so, under what conditions are they formed?

Recent discoveries suggest an affirmative answer to the first question. In 1996, both British and US expeditions to the slow-spreading Mid-Atlantic Ridge found remarkable seafloor edifices, each of which appears to have originated by long-lived slip on an individual normal fault. These features, which we term "megamullions," have two distinctive characteristics: first, a domelike or turtleback shape extending over a diameter of some 15 to 30 kilometers, and second, conspicuous grooves or corrugations (mullions) that formed as part of the faulting process and that parallel the direction of fault slip over the domed surface. (See figure above.) We have interpreted the megamullions as footwall blocks, that is, blocks ex-

humed from beneath normal faults. (See figure below.) In the case of megamullions, these faults have been unusually long-lived and areally extensive, and we refer to them as "detachment faults." Once megamullions were recognized, our subsequent study of existing, detailed multibeam bathymetric data has identified a total of 17 of these features



Jack Cook

Interpreted development of a megamullion near the end of a spreading segment during a period of amagmatic extension. Development begins when a detachment fault first forms following a magmatic episode of seafloor spreading, and it ends with abandonment of the detachment when a new fault breaks through rift-axis crust that is weakened by renewed magmatism.

between about 21° N and 31° N on the Mid-Atlantic Ridge, and a number of other megamullions have been recognized where strong tectonic extension occurs on slow- to intermediate-spreading mid-ocean ridges in the Indian Ocean.

Each detachment fault that forms a megamullion has three notable features: a breakaway zone where the fault began, the exposed fault surface that rides over the megamullion dome, and a termination, which usually is marked by a valley and adjacent ridge. By identifying breakaway and termination ages from dated seafloor magnetic anomalies, we can establish that the faults forming the North Atlantic megamullions accommodated slip for periods between 1.0 and 2.6 million years,

outside-corner (OC) crust on the opposite side of the spreading axis. This seems to be best explained by consistent orientation of faults dipping from inside corners toward outside corners; in this way the upper crust (hanging wall) is frequently stripped from the inside-corner footwall. However, this process cannot be continuously occurring on a single fault. If it were, all inside corners would exhibit megamullions (but only a small percentage do), and they would almost exclusively expose mantle rocks (which they do not). Rather, it appears that a single fault is normally active for only a short period of time (a few tens to hundreds of thousand of years) before it is abandoned and replaced by a new fault closer to the spreading axis.



Brian Tucholke

Domed metamorphic core complexes analogous to oceanic megamullions can develop in continental extensional regimes. In southern California, the gently dipping Whipple detachment fault separates a footwall core complex (gray, highly deformed mid-crustal mylonites and chloritized breccias) from the overlying hanging wall (dark brown, Miocene volcanics). In the foreground, Eric Frost of San Diego State University outlines the tectonic framework to members of the JOIDES (Ocean Drilling Project) Tectonics Panel.

with an average period of 1.5 million years. The original dip of the faults is uncertain, but they probably dipped at up to about 45°, much like most seismically active normal faults presently observed at the axes of mid-ocean ridges. With this dip, the faults would have exhumed a full 6-kilometer-thick crust and even exposed the underlying mantle within less than a million years. As these rocks are drawn out from beneath the fault, the footwall “rolls over,” laying out the geological cross-section across the surface of the megamullion. The rollover also flexes the brittle footwall much like bending a wooden ruler—the upper part of the footwall block is under tension and new normal faults break through the detachment surface.

Under what conditions do these long-lived faults develop? In terms of their position on the seafloor, all megamullions identified thus far appear near segment ends at inside-corner (IC) locations (that is, within the bights between the actively slipping sections of ridge-axis discontinuities and the spreading axis). Geophysical data and recovered rock samples show that ocean crust at inside corners of slow-spreading ridges is intermittently thin or missing compared to relatively normal thickness,

What, then, promotes slip on a single fault for periods of up to 2 million years or more? And what eventually causes the fault to be abandoned? Clearly, for a fault to remain active it must be weak in comparison to adjacent crust where another fault might otherwise nucleate. Recent laboratory studies have demonstrated changes in deformation mechanism at sub-seafloor depths where faults in the brittle lithosphere flatten out into zones of plastic deformation in hotter, deeper rocks. These changes weaken the rock by a factor of ten or more compared to surrounding, unfaulted rocks, and they thus promote slip in the shear zone. Slip probably is also enhanced by the occurrence of weak serpentinites along faults at shallower levels within the brittle lithosphere. Serpentinites form as seawater percolates down fractures and reacts with ultramafic rocks in the lower crust and upper mantle at temperatures ranging from about 100° to 500°C.

These kinds of weakening, however, are not the entire answer to the question of fault longevity because they probably occur on many (if not most) faults in slow-spreading crust, whereas truly long-lived faults are few and far between. A more complete explanation can be devised if we consider the temporal variability of magmatism at the spreading axis. Episodes of magmatism are known to occur at time scales of tens to hundreds of thousands of years at slow-spreading ridges, and recent analysis of gravity data over ridge flanks also indicates a predominant cycle at a period of two to three million years. Megamullions consistently correlate with the parts of these longer cycles where the gravity data indicate the presence of thin crust and predominantly amagmatic extension. Thus, it appears that persistent slip on a fault occurs while the spreading axis is relatively cold, but that when magmatism is renewed, it heats and weakens the lithosphere, new faults form, and the long-lived fault is abandoned. The relative rarity and the locations of megamullions

suggest that completely amagmatic extension is not common even in slow-spreading crust, and when it occurs it is restricted mostly to segment ends near ridge-axis discontinuities.

Windows of Opportunity

The cross sections through the crust and into the upper mantle that appear to be laid out across the surface of megamullions offer exciting new windows of opportunity finally to sample the oceanic lithosphere in detail. Marine geologists are now proposing to drill a series of half- to one-kilometer-deep holes, aligned in the direction of fault slip across the surfaces of megamullions. From these cores, we should be able to construct a composite, but relatively complete, picture of the entire crust-mantle section, without ever having to drill the 6 kilometers or more that would be required to reach the mantle beneath normal-thickness ocean crust.

There is, however, much to be done before the drilling occurs. A few samples have been obtained from megamullions, and as expected they include lower-crustal and upper-mantle rocks. Nonetheless, most of our interpretations are based on remotely sensed data such as gravity and bathymetry, together with models of the faulting process. Detailed surveys and sampling with deep-towed instruments and submersibles like *Alvin* are needed fully to document the geology of the outcrops and to select optimum locations for drilling. This mapping and sampling will also provide critical information for correlating data between drill holes and to understand the three-dimensional internal structure of the crust and mantle.

In addition to providing lithospheric cross sections, megamullions have the potential to yield significant insights into other outstanding geological problems. For example, it has long been thought that the primary source of marine magnetic anomalies lies in the upper, extrusive section of the oceanic crust. Yet, at megamullions, where this layer is thought to be missing, perfectly normal magnetic anomalies usually are developed. Either we are grossly mistaken in our interpretation of these features, or else the lower part of the ocean crust contains a substantial magnetic signature. Near-seafloor magnetic studies and laboratory analyses of magnetization in recovered rock samples will resolve this question.

Although the focus here has been on oceanic lithosphere, we also can benefit from and contribute to the study of tectonics in continental crust (see photos on these two pages). Megamullions have dimensions, shape, and an apparent mode of origin



Brian Tucholke

via long-lived detachment faulting that are very similar to those of “metamorphic core complexes” exposed in extensional mountain belts such as those found in the southwestern United States. In these areas, domed core complexes have exhumed rocks from some 15 kilometers deep in the continental crust, and their structure and deformation history have been studied extensively for more than two decades. Cross-pollination of insights gained from both the continental and oceanic realms will allow us to develop a much more comprehensive understanding of extensional tectonism and the intriguing exposures of deep lithosphere both on land and in the ocean basins.

This mid-ocean ridge research has been supported by the National Science Foundation, the Office of Naval Research, and WHOI’s Andrew W. Mellon Foundation Endowed Fund for Innovative Research. The author is indebted to colleagues Jian Lin, Marty Kleinrock (Vanderbilt University), Greg Hirth, Henry Dick, and Joe Cann (University of Leeds, UK) for stimulating discussions about tectonism in slow-spreading crust, and to Eric Frost (San Diego State University) and Kip Hodges (MIT) for superb field exposition of extensional tectonics in the Basin and Range.

Born and raised in the natural geological laboratory known as the Black Hills of South Dakota, Brian Tucholke has been a geologist from the time he first crawled off his baby blanket and grabbed a fistful of dirt. As one of the Ph.D. students entering the MIT/WHOI Joint Program in its inaugural year, he (mostly) gave up the bedrock stability of the western mountains for the rolling sea, and he has since been on more than 25 oceanographic research cruises to investigate the flow of abyssal currents, seafloor sedimentation patterns, the paleoceanographic history of ocean basins, the structure and evolution of continental margins, and the tectonics of mid-ocean ridges. The mark of his passage can often be seen in the imprint of his cowboy boots, several decrepit pairs of which he has buried at sea in oceans ranging from the North Atlantic to the Bellingshausen Sea off Antarctica.

Continental metamorphic core complexes are often, and appropriately, called “turtlebacks.” Here in Death Valley, the domed, gray core complex of mid-crustal mylonites and breccias at right is separated from brown upper crustal volcanics and sediments by the north-west-dipping Copper Canyon detachment fault. Width of view is about a kilometer along the contact with the alluvial plain in the foreground.



How to Build a Black Smoker Chimney

Alvin's manipulator reaches toward a black smoker chimney, seen through the sub's viewport, at 17°S on the East Pacific Rise. Hot hydrothermal fluids surge through the chimney at velocities of 1 to 5 meters per second. The "black smoke" consists of an abundance of dark, fine-grained, suspended particles that precipitate when the hot fluid mixes with cold seawater.

The Formation of Mineral Deposits At Mid-Ocean Ridges

Margaret Kingston Tivey

Associate Scientist, Marine Chemistry & Geochemistry Department

Diving along the mid-ocean ridge at 21°N on the East Pacific Rise, scientists within the deep submersible *Alvin* peered through their tiny portholes two decades ago to see an astonishing sight: Clouds of billowing black "smoke" rising rapidly from the tops of tall rocky "chimneys." The "smoke" consisted of dark, fine-grained particles suspended in plumes of hot fluid, and the "chimneys" were made of minerals that were rich in metals. Using specially designed fluid bottles and temperature probes, *Alvin* took samples of these black smoker chimneys, as well as the 350°C fluids venting

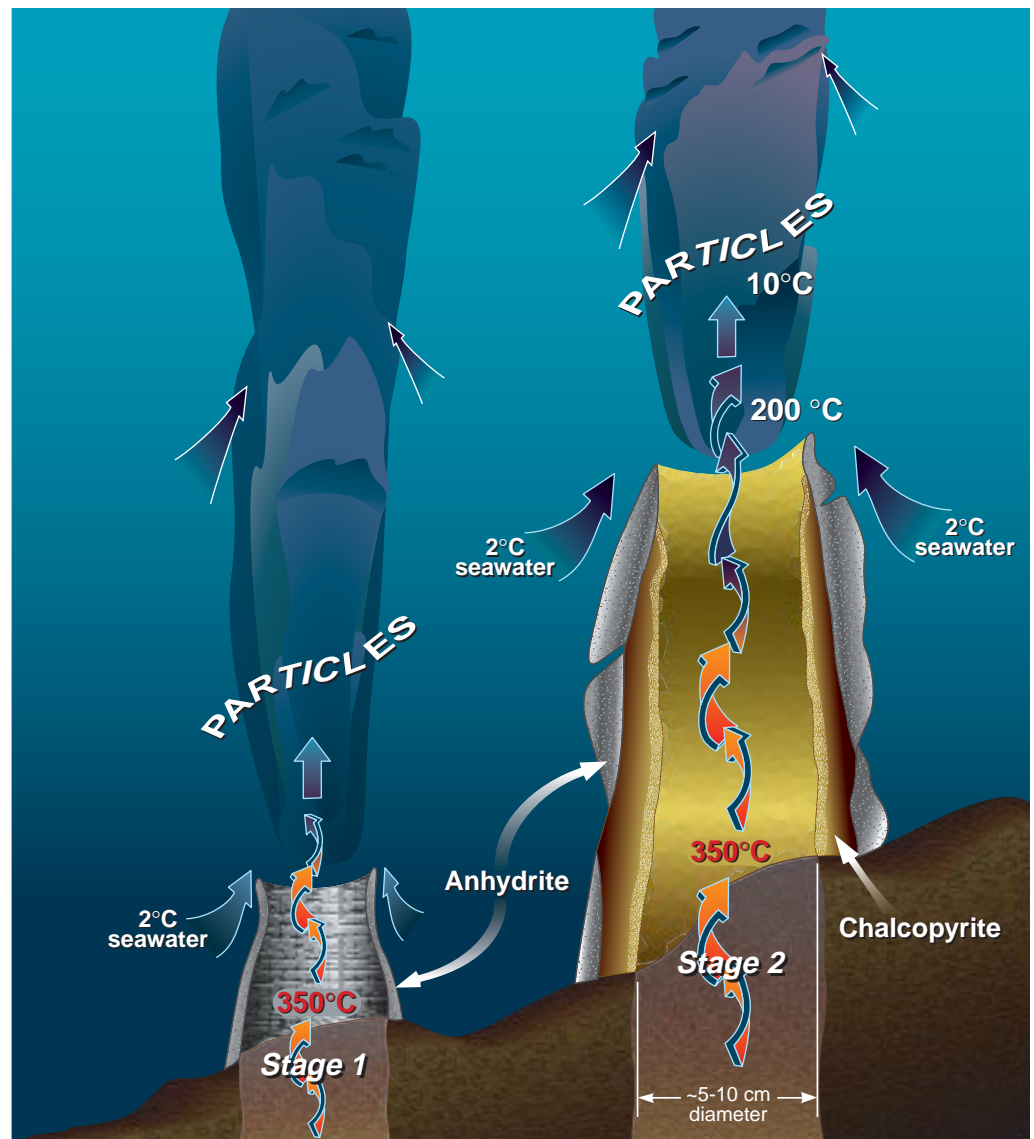
from them. Since then, scientists have observed and sampled numerous active vent sites along portions of the mid-ocean ridge in the Atlantic and Pacific Oceans, and in back arc basins in the Pacific Ocean. It has become abundantly clear that these high-temperature seafloor hydrothermal systems are the analogs to systems that created some of the world's economically valuable mineral deposits, including some that have been mined on land. In Cyprus and Oman, for example, ore deposits of millions of tons are found in ophiolites, portions of ancient seafloor thrust onto land by tectonic forces.

Scientists can gain much insight into hydrothermal processes through detailed studies of these exposed areas of fossil systems, but only by investigating active systems can they simultaneously examine hydrothermal fluids and the corresponding mineral deposits created by them. By analyzing these fluids and deposits, we have been able to formulate models to explain how submarine mineral deposits, from seafloor chimneys to great subseafloor depths, are initiated and how they grow in their early stages.

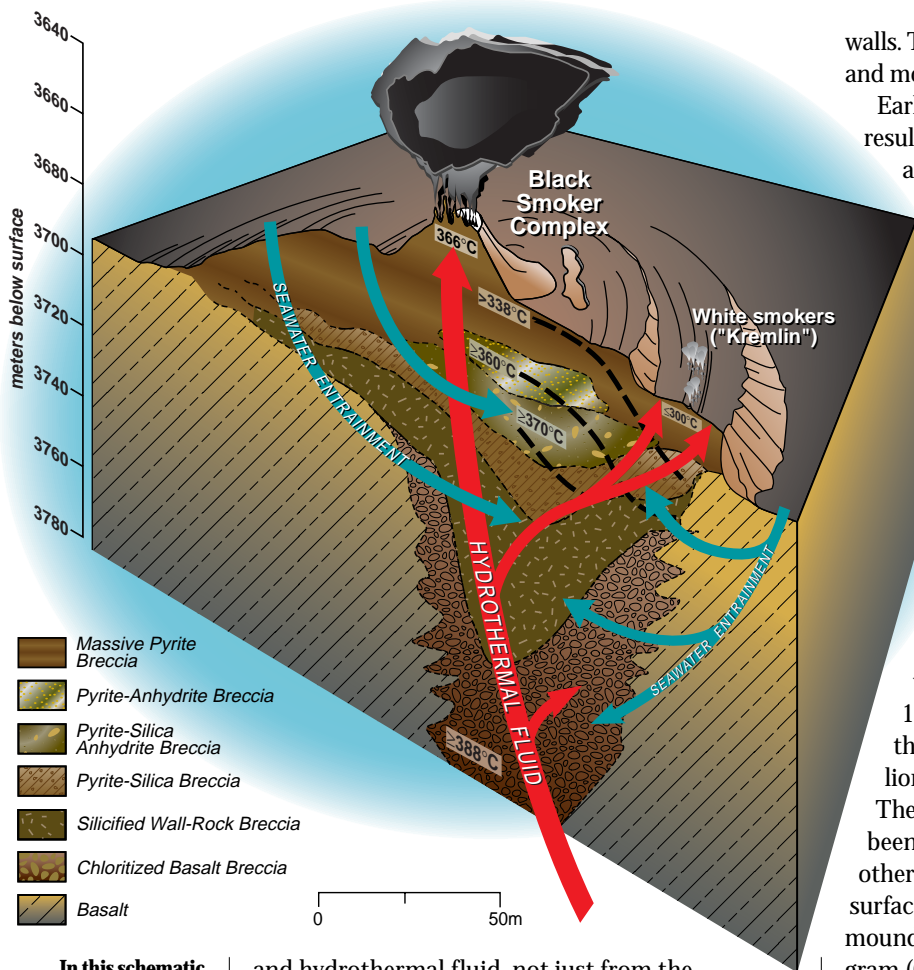
One of the most fascinating aspects of black smoker chimneys is how rapidly they form. They have been measured to grow (after upper parts of the chimneys are razed by sampling) as fast as 30 centimeters per day. Examination of young chimney samples, under the microscope and by X-ray diffraction, revealed that the earliest stage in the creation of a black smoker chimney wall involves precipitation of a ring of a mineral called anhydrite. The ring forms around a jet of 350°C fluid, which exits the seafloor at velocities of between 1 and 5 meters per second. Anhydrite, or calcium sulfate (CaSO_4), is an unusual mineral because it is more soluble in seawater at low temperatures than at high temperatures. Seawater contains both dissolved Ca^{2+} and SO_4^{2-} ions, and when it is heated to 150°C or greater, the ions combine and anhydrite precipitates. Hydrothermal fluids contain little or no sulfate, so the origin of the sulfate in the precipitated anhydrite is seawater. Calcium, however, is present in both seawater and hydrothermal fluid. That made it more difficult at first to determine whether the initial anhydrite chimney wall formed solely from seawater that was heated by hydrothermal fluids, or from the mixing of cold, sulfate-rich seawater with hot, calcium-rich hydrothermal fluid.

Strontium, which is present in seawater and hydrothermal fluid, was used to investigate this problem. Strontium has the same charge as calcium and a number of different, easily measurable isotopes. (Isotopes are

elements having the same number of protons in their nuclei, but different numbers of neutrons. Thus they share chemical properties but have slightly different physical properties.) Strontium can readily take the place of calcium in the crystalline lattice that forms when anhydrite precipitates. The concentration of strontium, as well as the ratio of two of its isotopes, strontium 87 and strontium 86, were measured in both vent fluid and in seawater. Because the ratio of strontium 87 to strontium 86 is higher in seawater than in hydrothermal fluid, it is possible to determine whether the source of the strontium (substituting for calcium in newly formed anhydrite grains) is seawater or vent fluid. The answer is both: Anhydrite walls form from the turbulent mixing of seawater



During Stage 1 of black smoker chimney growth, hot, calcium-rich vent fluid mixes turbulently with cold, sulfate- and calcium-rich seawater, resulting in precipitation of a ring of calcium sulfate (anhydrite). Metal sulfides and oxides carried in the hot fluid also precipitate rapidly during the mixing process, forming a plume of dark particles above the vent. During Stage 2 of chimney growth, the initial chimney wall of anhydrite forms a surface on which chalcopyrite (copper-iron sulfide) begins to precipitate and plate the inner chimney wall. Mixing of seawater and hydrothermal fluid components across the porous wall by advection and diffusion results in the deposition of zinc, copper-iron, and iron sulfides in the interstices of the wall, which gradually makes the chimney less porous and more metal-rich.



In this schematic drawing of the TAG active hydrothermal mound, hydrothermal fluid rises rapidly and exits the mound at the Black Smoker Complex. Cold calcium- and sulfate-rich seawater is entrained into the mound, where it mixes with hydrothermal fluid. The mixing causes anhydrite, pyrite, and chalcopyrite to precipitate inside the mound. This precipitation increases the acidity of the hydrothermal fluid. Zinc and other elements, such as silver, gold, and cadmium, dissolve in this acidic fluid, allowing them to be carried by the white smoker fluid to the edges of the mound at the "Kremlin" area. Here the cooler temperatures within white smoker chimney walls cause the elements to precipitate.

and hydrothermal fluid, not just from the rapid heating of seawater.

During this mixing, other processes occur during early stages of chimney growth. Metal sulfides and oxides (zinc sulfide, iron sulfide, copper-iron sulfide, manganese oxide, and iron oxide) precipitate from the vent fluids as fine-grained particles, most of which form a plume of "smoke." Because bottom seawater is denser than the mix of seawater and hydrothermal fluid in the plume, the plume rises some 200 meters above the ridge to a level of neutral buoyancy. Some particles form close to the chimney and become trapped within and between grains of anhydrite within the nascent chimney walls. These particles give the anhydrite, which is white in its pure form, a gray to black color. Copper-iron sulfide (chalcopyrite, or CuFeS_2) begins to precipitate and plate the inner surface of the chimney. The evolving chimney walls are thin, ranging from less than a quarter of an inch to a few inches, but on either side of them are large gradients of pressure, temperature, and concentrations of elements. Aqueous ions, including copper, iron, hydrogen sulfide, zinc, sodium, chloride, and magnesium, are transported from areas of high to low concentrations (by diffusion). These elements also are carried by fluids flowing back and forth across the wall from areas of high to low pressure (by advection). As a result of these processes, zinc sulfide, iron sulfide, and copper-iron sulfide precipitate in the interstices of the chimney

walls. The chimney walls thus become less porous and more metal-rich over time.

Early examinations of black smoker chimneys resulted in a model of chimney growth that is still accepted nearly 20 years later. But in terms of size and ore grade, black smoker chimneys are not important mineral deposits. Most of the metals are lost into the plume that rises into the water column above the vents and is dispersed. In the last decade, the focus of study has shifted to larger deposits present along mid-ocean ridges.

In 1985, scientists aboard Woods Hole Oceanographic Institution's *Atlantis II* discovered hydrothermal vents at the Trans-Atlantic Geotraverse (TAG) active mound, the single largest known active mineral deposit along the mid-ocean ridge. Roughly circular in plan view, the TAG site has a diameter of about 150 meters and rises some 50 meters above the seafloor, with an estimated mass of 3 million tons. TAG has been intensively sampled. The *Alvin*, *Mir*, and *Shinkai* submersibles have been used to recover vent fluids, chimneys, and other hydrothermal precipitates from the mound surface. And in 1994, 17 holes were drilled into the mound during Leg 158 of the Ocean Drilling Program (ODP). Drillcore was recovered from five mound areas to a maximum depth of 125 meters below the seafloor.

As in studies of black-smoker chimneys, the combination of vent fluid data and examinations of anhydrite played an important role in determining the processes involved in growth of the large TAG mineral deposit. In 1990, two distinct fluid compositions were observed to be exiting the TAG mound. From the so-called Black Smoker Complex in the northwest area of the mound, 366°C black smoker fluid billowed from an aggregation of chimneys in a huge black plume that shrouded nearly the entire complex. Approximately 70 meters southeast of this complex, however, clear fluid with temperatures of less than 300°C emanated from an area called the Kremlin, named for its 1- to 2-meter-high chimneys with their distinctive, onion-shaped Byzantine cupolas. The mineral composition of the black smoker chimneys was very similar to those of black smokers at other mid-ocean ridge vent sites. The chimneys forming from the cooler white smoker fluid, however, were quite different, containing significant amounts of zinc, as well as cadmium, silver, and gold. Analyses of the white smoker fluids indicated that they were more acidic and contained less copper, iron, calcium, and hydrogen sulfide, but 10 times more zinc, than the hotter black smoker fluids. However, concentrations of other elements, such as potassium, were identical, suggesting that

the two fluids were related to one another.

A hypothetical series of steps was soon developed to explain these observations. The deficits of copper, iron, and hydrogen sulfide in the cooler white smoker fluid could best be explained by the precipitation of copper-iron sulfide and iron sulfide (that is, chalcopyrite and pyrite) *within* the mound. In addition, it was theorized that precipitation of anhydrite *within* the mound could explain the lower calcium concentrations in white smoker fluids. To trigger the deposition of sulfates and sulfides inside the mound, sulfate-rich seawater would have to percolate down into the mound and mix with the hotter hydrothermal fluid. The precipitation of sulfides would release hydrogen ions, making white smoker fluid more acidic. The increased acidity, in turn, would cause metals in the mound, such as zinc, cadmium, silver, and gold, to dissolve. Once dissolved in the fluid, these so-called “remobilized” elements could be transported toward the upper edge of the mound. This would explain the excess zinc observed in white smoker fluid. At the seafloor, the white smoker fluid, rich in remobilized metals, confronts 2°C seawater just outside the chimney wall. Crossing this thermal gradient, the fluid cools, and some metal-rich minerals precipitate. This process, known as “zone refinement,” explains how some ore deposits are separated into large-scale zones containing different metals, with copper in the center of the deposits, for example, and zinc at the edges.

To determine whether the scenario described above was reasonable, we used geochemical modeling calculations, which take into account the thermodynamics of a range of different chemical reactions at high temperatures. The theoretical reactions had to reproduce the already-well-documented composition of the less-than-300°C fluid from combinations of the 366°C fluid and seawater. These calculations demonstrated that the composition of the cooler white smoker fluid we observed could theoretically result from mixing 86 percent black smoker fluid with 14 percent seawater, which would result in the precipitation of 19 parts anhydrite, 8 parts pyrite, and 1 part chalcopyrite within the mound, as well as the remobilization of zinc and other metals by the resultant acidic fluid.

These predictions were put to the test when the TAG mound was drilled in the fall of 1994. One of ODP Leg 158’s major findings was that significant amounts of anhydrite are present throughout the mound. Anhydrite has not been seen in analogous ophiolite structures probably because it dissolves at lower temperatures and essentially has disappeared from land-based deposits. But anhydrite was recovered from three of the five sites drilled at TAG. It was present at the base of the deepest hole drilled at the TAG site, to a depth of 125 meters below the seafloor. The drilling revealed that the mound contained wide, complex, anhydrite-rich

veins, ranging in size from 1 millimeter to 1 meter wide, which formed as anhydrite precipitated in cracks within the mound.

The discovery of anhydrite confirmed the prediction that seawater was entering and traveling through the mound. It also let us determine the proportions of seawater that were mixing with hydrothermal fluid within the mound. Analyses of strontium isotopes from anhydrite grains recovered from various depths in the mound demonstrated that anhydrite was forming from mixtures that



Tom Kleindinst

ranged from 99.5 percent seawater and 0.5 percent hydrothermal fluid to 52 percent seawater and 48 percent hydrothermal fluid.

Samples of anhydrite grains recovered from drilled cores were also used to determine the temperature and salinity of fluids at various points within the mound. When mineral grains form, small amounts of the fluid from which they are forming can be trapped and enclosed within the precipitating grain. As a result, small cavities can form within the mineral,

Author Margaret Tivey examines the top of a spire of a black smoker chimney retrieved by *Alvin* from the East Pacific Rise at 17°S.

Thin-section samples of chimney wall specimens, examined under a microscope, reveal metal sulfide particles (black) embedded in and around anhydrite crystals (clear).

which may contain one or more phases (liquid, vapor, or solid). These are called fluid inclusions. The cavities can range in size from about 1 micron to greater than 1 millimeter, though 3- to 20-micron inclusions are most common. The anhydrite grains from the TAG mound all contained abundant fluid inclusions with two phases: liquid and a vapor bubble.

We analyzed fluid inclusions within mineral grains by using a heating-freezing stage attached to a high-magnification microscope. The salinity is determined by freezing the fluid within the inclusion at temperatures of less than -50°C and then slowly heating until the last ice melts. The temperature of final melting is a function of the salt content in the fluid. The temperature of the fluid when it was trapped within the mineral also can be determined by heating the fluid inclusion and measuring the temperature at which the vapor bubbles disappear. With adjustments for undersea pressures, measurements of fluid inclusion trapping temperatures from a number of different anhydrite grains recovered from within the TAG mound indicated very high temperatures (greater than 337°C) throughout most of the mound. At depths greater than 100 meters below the seafloor, trapping temperatures were in excess of 380°C .

The combination of strontium-isotope and fluid-inclusion analyses of TAG anhydrite grains not only demonstrated that large amounts of seawater are being entrained into the mound, they also showed that anhydrite (and chalcopyrite and pyrite) precipitated in the mound from seawater-hydrothermal fluid mixtures that are greater than 50 percent seawater. That led to a dilemma and to another discovery. The dilemma was that our geochemical modeling calculations predicted that if the mixing proportions were greater than 50 percent seawater, and if mixing alone determined the temperature of the fluids in the mound, the fluid temperatures in the mound should be relatively low (5° to 250°C). Our fluid inclusion measurements, however, indicated that the anhydrite grains were nearly all precipitating at much higher temperatures, 187°C to 388°C .

The logical conclusion is that the seawater and seawater-hydrothermal fluid mixtures that are entering and travelling through the mound are being heated by conduction. Hot black smoker fluids are flowing rapidly along a direct, highly focused route up through the mound to the Black Smoker Complex. Drilling within the mound revealed extensive accumulations of breccia—rocks made of sulfide-rich fragments that conduct heat well. So it is reasonable to conclude that cold seawater

is being conductively heated as it flows through channels bounded by breccias. If enough seawater is being heated in this way, black smoker fluid may be cooled slightly as it rises through the mound to the Black Smoker Complex—from the 388°C temperatures found in the anhydrite grains near the base of the mound to the 366°C temperatures of the exiting black smoker fluids.

Results of drilling revealed other important information on the internal structure of the TAG active mound. By dating mound materials, it is possible to

reconstruct a history of the mound, showing that it has undergone repeated episodes of high-temperature fluid flow, punctuated by quiescent periods, over a roughly 20,000-year interval.

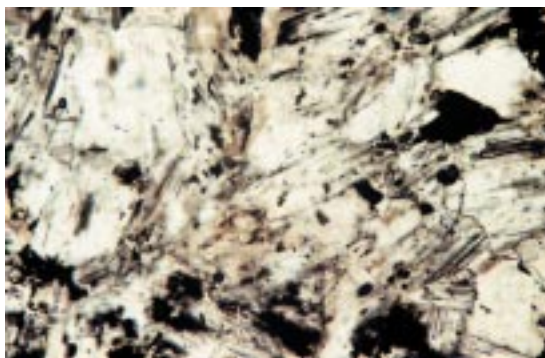
When the high-temperature fluid flow ceases, the anhydrite dissolves, and the chimneys that the

anhydrite supports collapse, scattering fragments of rock. When high-temperature fluid flows resume and percolate through these fragments, anhydrite precipitates and serves as a matrix that cements together fragmented chimney pieces and mound materials into breccia deposits. Textures within the TAG breccias indicate that there have been multiple cycles of mound material reworking—a likely consequence of repeated episodes of anhydrite deposition and dissolution.

Information from the TAG mound shows how this kind of intermittent activity can, over long periods of time, result in the gradual formation of a large hydrothermal mineral deposit similar to the ore bodies preserved in Cyprus. Studying the large TAG active mound has greatly increased our understanding of how large mineral deposits like these can form.

Meg Tivey's research on hydrothermal deposits has been funded through the National Science Foundation and the Joint Oceanographic Institutions/US Science Advisory Committee. Her work on the TAG active mound has benefited from collaborations with many scientists, including Susan Humphris and Geoffrey Thompson (WHOI), Rachel Mills (University of Southampton), and Mark Hannington (Geological Survey of Canada).

Meg Tivey chose to major in geology after taking a course with five field trips to local beaches and fault zones. She then worked as a physical science technician at the US Geological Survey before deciding to pursue graduate studies in marine geology at the University of Washington. She now specializes in studies of active seafloor hydrothermal systems. Her current projects include examining the formation of polymetallic sulfide deposits, continuing work on linking measured vent fluid compositions to observed mineralogy of vent deposits, using X-ray computed tomography (CAT scans) to examine seafloor sulfide samples in three-dimensions, and working with engineers to build instruments capable of measuring temperatures and flow rates on the seafloor in high-temperature and low-pH fluids.



Tom Klemdinet